ALMA MATER STUDIORUM - UNIVERSITÀ DI BOLOGNA

FACOLTA' DI INGEGNERIA

CORSO DI LAUREA IN CIVIL ENGINEERING

DIPARTIMENTO
DICAM

TESI DI LAUREA

in
ADVANCED DESIGN OF STRUCTURES

THE COLLAPSE OF THE TWIN TOWERS

CANDIDATO

Carlotta Malavolti

RELATORE:

Chiar.mo Prof. Marco Savoia
Università di Bologna

CORRELATORE

Chiar.mo Prof. Rene B. Testa
Columbia University
in the city of New York

Anno Accademico [2010/2011]

Sessione [III]

Contents

Introduction

The collapse of the Twin Towers is among the worst building disasters of the world and over 3000 people lost their lives on September 11, 2001.

This work focuses on the structural analysis of the collapse of the external tube of the Towers and specifically on the role of the interconnections of the panels that made up the tube in the stability of the tube walls when support is lost from the building floors. The Towers in fact were built as 2 boxes one inside the other: the core and the external tube. The report begins with an overview of the structure of the buildings, giving special attention to the three main parts of the structure (the core, the tube and the floors) and a summary of the outlines of the collapse (the successions of the events and the contribution of the fire to the collapse).

The analysis studies the buckling of one face of the external tube of the Twin Towers. First of all the panels, the main structural components of the tube, are described. A finite element model solved with the software SAP2000 is used to analyze this feature.

The results obtained are compared with simple cases in order to check the reliability of the analysis performed. Conclusions regarding the role of panel interconnections are presented.

Chapter 1 The structure

The World Trade Center 1 and World Trade Center 2 were designed by Minoru Yamasaki as the chief architect and the structural engineering were John Skilling, Helle, Christiansen, Leslie Robertson**.**

The complex consisted of seven buildings, dominated by the twin 110-story towers rising more than 1,360 feet (415 meters) above an open plaza.

Each building had a 63.1m by 63.1m square floor plan with corner chamfered 2.1m. The service core was rectangular with dimensions of approximately 26.5m by 41.8m.

A total of 59 perimeter columns were present along each face of the building. In alternate stories an additional column was present at the center of each chamfered building corner [1,Chapter 2].

In this design, the support structure is spread throughout the entire building. There were built long "tubes," where all the support columns were around the outside of the building and at the central core of the building. Each tower was a box within a box, joined by horizontal trusses at each floor.

The outer box, measuring 208 feet by 208 feet (63x63 m), was made up of 14-inch (36-cm) wide steel columns, 59 per building face, spaced 3 feet (1 m)apart. On every floor above the plaza level, the spaces between the columns housed 22-inch (56-cm) windows. Metal beams are settled end to end to form vertical columns, and at each floor level, these vertical columns are connected to horizontal girder beams.

The support columns were all internal, so the outside of the building doesn't have to hold up anything but its own weight.

The columns were covered with aluminum, giving the towers a distinctive silver color. The inner box at the core of each tower measured about 135 feet by 85 feet (41x26 m). Its 47 heavy steel columns surrounded a large open area housing elevators, stairwells and restrooms.

This design had two major advantages:

- First of all, it gave the building remarkable stability. In addition to supporting some of the vertical load (the weight of the building), the outer steel columns supported all of the horizontal forces acting on the tower (the force of the wind). This meant the inner support structure was completely dedicated to the huge vertical loads.

- Secondly, with the support structure moved to the sides and center of the building, there was no need to space bulky columns throughout each floor.

  The vertical support columns at the core of the building went down below the bottom floor, through the basement structure, to the spread footing structure below ground. In the spread footing design, each support column rested directly on a cast-iron plate, which sited on top of a grillage. The grillage is basically a stack of horizontal steel beams, lined side by side in two or more layers. The grillage rested on a thick concrete pad poured on the solid bedrock deep underground. This pyramid shape distributed the concentrated weight from the columns over a wide, solid surface. With the steel in place, the entire structure was covered with concrete [4].

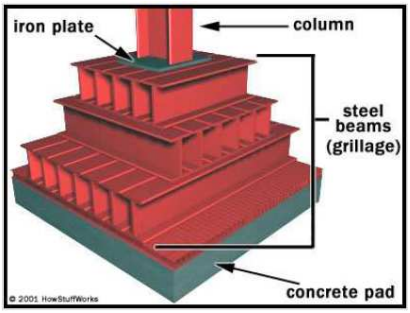

Figure 1. Basic spread footing design. 2002 Howstuffworks “The World Trade Center Tube

Near the base of each tower, at the plaza level, the narrowly spaced perimeter support columns rested on "column trees." The column trees spread the weight from the narrowly spaced columns over thicker columns spaced about 10 feet (3 m) apart. Each of these columns rested on additional, smaller support footings in the foundation [4].

The buildings were formed by three main parts:

- The core
- The tube
- The decks and connector

1.1 The Core

The core of each tower measured about 135 feet by 85 feet (41x26 m) and it consisted of 47 columns.

The core consisted of 5 inches concrete fill on metal deck supported by floor framing of rolled structure shapes, in turn supported by combination of wide flange shape and box section column, some very large 14 inches wide and 36 inches deep.

Core columns were built in hollow sections up to 84th floor, made of A36 (fy=248MPa) steel grade, while above the 84th floor, rolled or welded I-shaped sections were used.

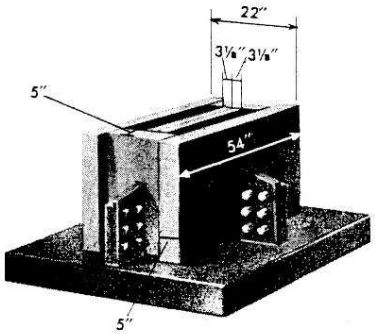

Figure 2. Rectangular box columns that in the upper stories transitioned into heavy rolled wide flange shapes. FEMA report 2000

Between 106th and 110th floors, a series of diagonal braces were placed into brace frame. These diagonal braces together with the building columns and floor framing formed a deep outrigger truss system that extended between exterior walls and across the building core framing. A total of 10 outrigger truss lines: 6 extending across the long direction of the core and 4 extending across the short direction of the core

[1, Chapter2].

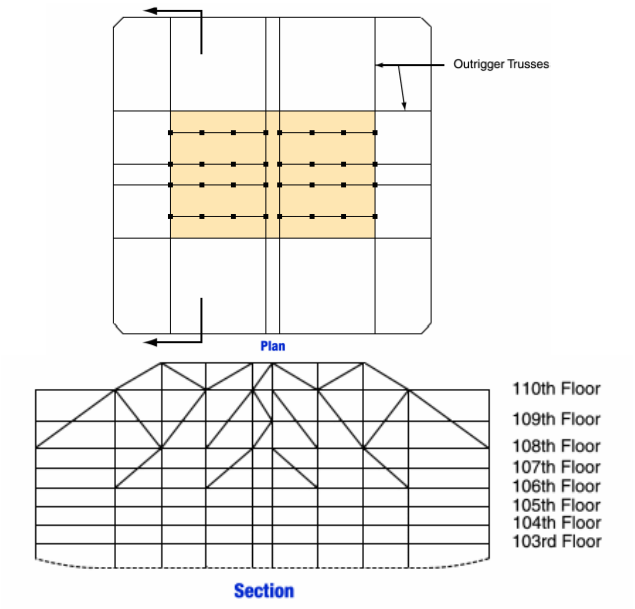

Figure 3.Outrigger truss sytem at tower roof. FEMA report 2000

Outrigger truss system provided stiffening of the frame for wind resistance, mobilized some of the dead load weight supported by the core to provide stability against wind load induced overturning, and also direct support for the transmission tower on WTC1. WTC2 didn't have transmission tower but the outrigger trusses were designed to support anyway this tower.

1.2 The Tube

The towers were high rise buildings constructed with the concept of a structural TUBE as lateral load resistance. The building perimeter is used to resist wind loads and the central core carries the gravity loads.

The tube behavior is achieved by arranging closely spaced columns connected by spandrel beams around the perimeter. The 4 exterior walls, acting as huge Vierendeel truss, formed a cantilever beam (Framed Tube) with square box section, internally braced by the floor system.

Vierendeel action occurs in rigid trusses that do not have diagonals; the stiffness is achieved through the flexural (bending) strength of the connected members. In the lower seven stories of the towers, where there were fewer columns, vertical diagonal braces were in place at the building core to provide this stiffness. This structural frame

was considered to constitute a tubular system. Under the effects of lateral wind loading the buildings behaved as cantilevered hollow structural tubes with perforated walls.
In each building the windward wall acted as a tension flange for the tube while the leeward acted as a compression flange. The side walls acted as the webs of the tube, and transferred shear between the windward and leeward walls through Vierendeel action [1,Chapter 2].

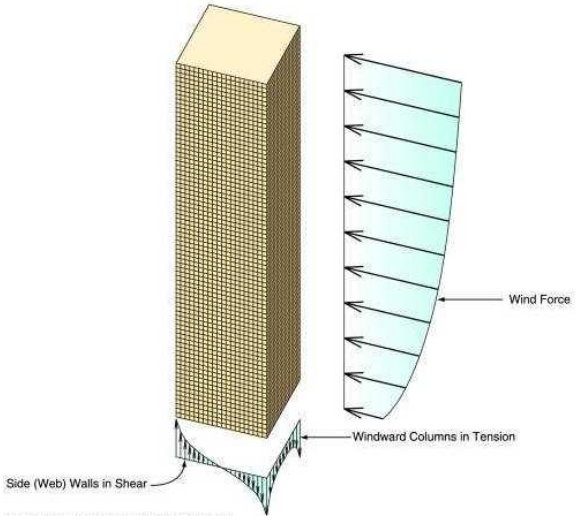

Figure 4 . Structural tube frame behavior. FEMA report 2000

The high efficiency of the Frame tube system in resisting wind loads, the use of viscoelastic damping system and the optimized employment of 12 different steel grades, allowed for reducing of 40% the structural steel. The weight of structural steel was 1,77 KN/m^2 This structural system allowed to keep the interior floor plan column free, increasing the net area of the building.
Another major design issue was: the control of differential axial shortening in the columns for preventing uneven settlement throughout the structure as loads were applied.

PERIMETER COLUMNS had built in sections made of 4 welded plates, for an area of 355.6 mm^2 section, placed at 1016 mm distance. Twelve grades of steel were used for these columns with yield strength ranging from 290 MPa to 690 MPa and different thickness along the height were adopted: 6.35mm-101.6mm.
Adjacent columns were linked at each floor level by high spandrel plates. The same steel grade adopted for the connected columns was typical adopted also for spandrels.

1.3 Floor System

Floor construction typically consisted of 4 inches of lightweight concrete on 1-1/2inch, 22 gauge non composite steel deck. In the core area, slab thickness was 5 inches. Outside the central core, the floor deck was supported by a series of composite floor trusses that spanned between the central core and exterior wall. Composite behavior with the floor slab was achieved by extending the truss diagonals above the top chord so that they would act like shear studs. Trusses were placed in pairs, with a spacing of 6 feet 8inches and spans of approximately 60 feet to the sides and 35 feet at the ends of the central core. Metal deck spanned parallel to the main trusses and was directly supported by continuous transverse bridging trusses spaced at 13 feet 4 inches and intermediate deck support angles spaced at 6 feet 8 inches from the tranverse trusses.

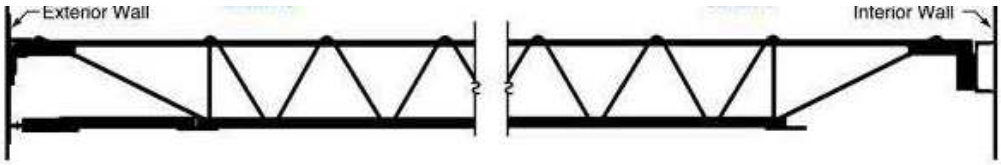

Figure 5. Exterior wall and interior wall FEMA report 2000

The combination of main trusses, transverse trusses, and deck support enabled the floor system to act as the grillage to distribute load to the various columns.

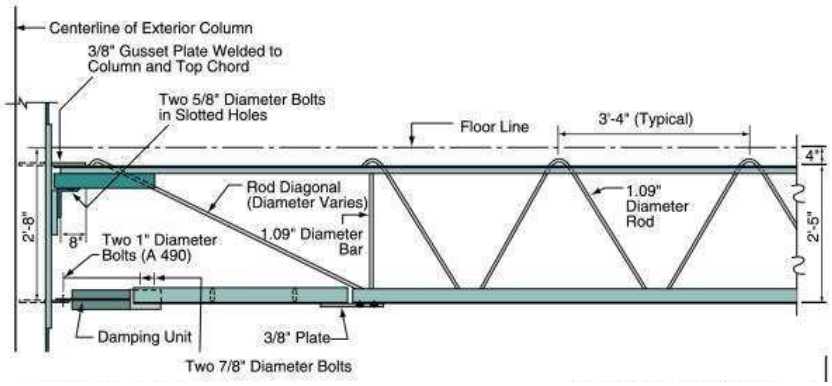

Figure 6. Exterior wall end detail. FEMA report 2000

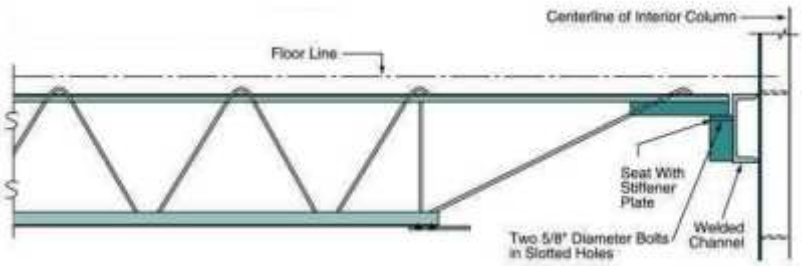

Figure 7. Interior wall end detail FEMA report 2000

At the exterior wall, truss top chords were supported in bearing off seats extending from the spandrels at alternate columns. Welded plate connections with an estimated ultimate capacity of 90 kips (620MPa) tied the pairs of trusses to the exterior wall for out of plane forces.

10,000 viscoelastic dampers in each building were extended between the lower chords of the joists and gusset plates, mounted on the exterior columns beneath the stiffened. The dampers are attached to only one end of each truss. These dampers were the first application of this technology in a high-rise building, and were provided to reduce occupant perception of wind-induced building motion [1,Chapter 2].

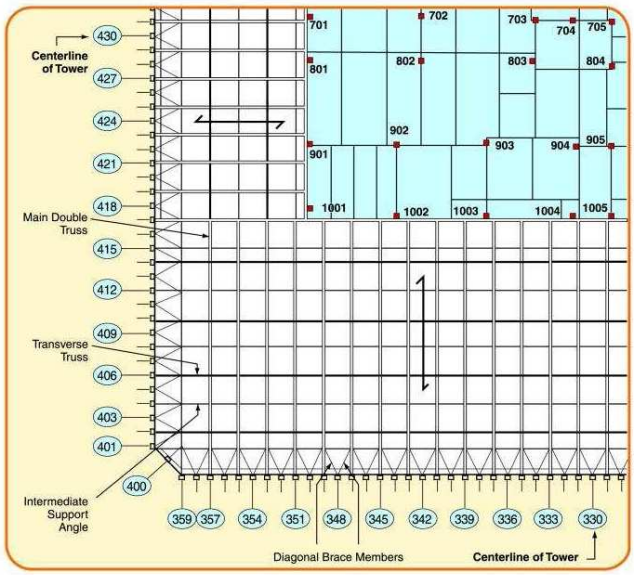

Figure 8. Representative framing plan, upper floors. FEMA report 2000

At the central core, trusses were supported on seats off a girder that crossed trough and was supported by the core columns. Out of plane connection was provided between the trusses and these girders.

Floors were designed for a uniform live load of 100 pounds per square foot (psf) over any 200-square-foot area with allowable live load reductions taken over larger areas. At building corners, this reached a uniform live load (unreduced) of 55 psf.

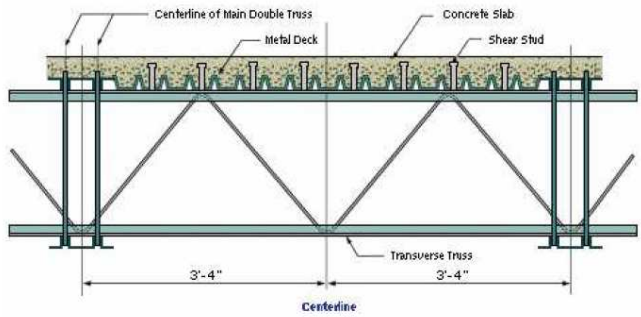

Figure 9. Cross-section through the main double truss, showing transverse truss (shear stud added). FEMA report 2000

Pairs of flat bars extended diagonally from the exterior wall to the top chord of adjacent trusses. These diagonal flat bars, which were provided with shear studs, provided horizontal shear, transferred between the floor slab and exterior wall.

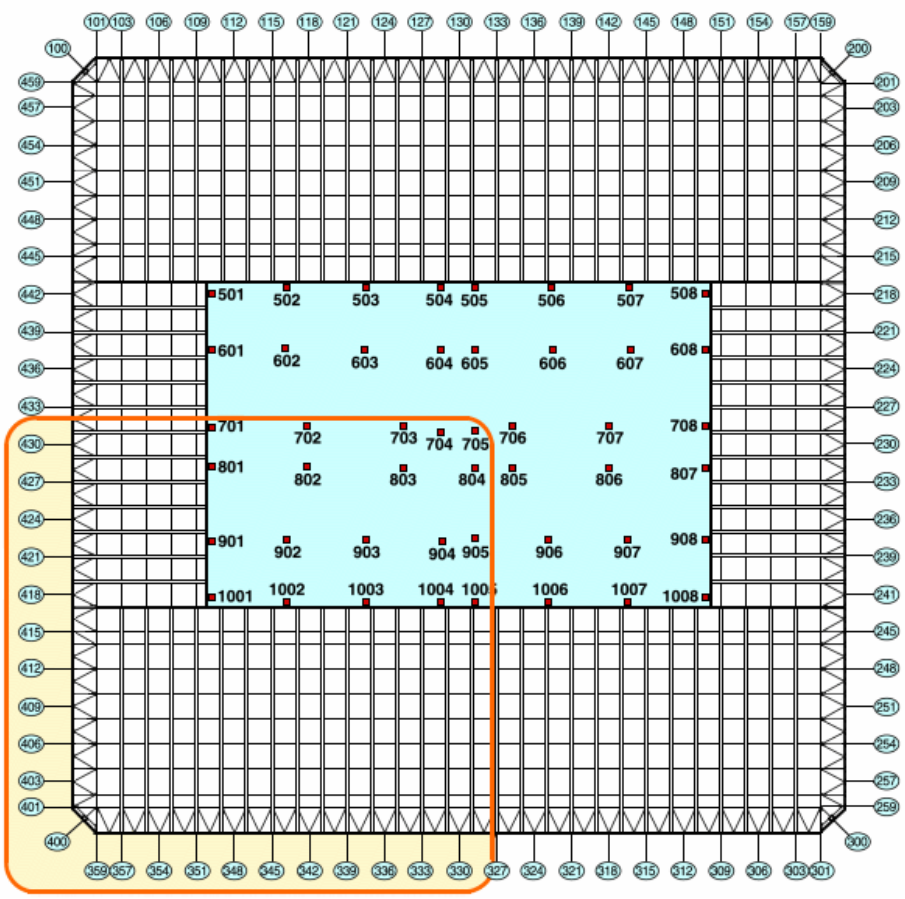

Figure 10. Representative structural framing plan, upper floors. FEMA report 2000

The diagonal flat bars are V-like features. There were 24 x 18 inch metal plates that were covered with shear studs and also set in the concrete slab. These plates, together with the 6 foot long diagonal bars and the welded and bolted truss connections, provided a strong connection between the floor slab and the perimeter wall [1,Chapter2].

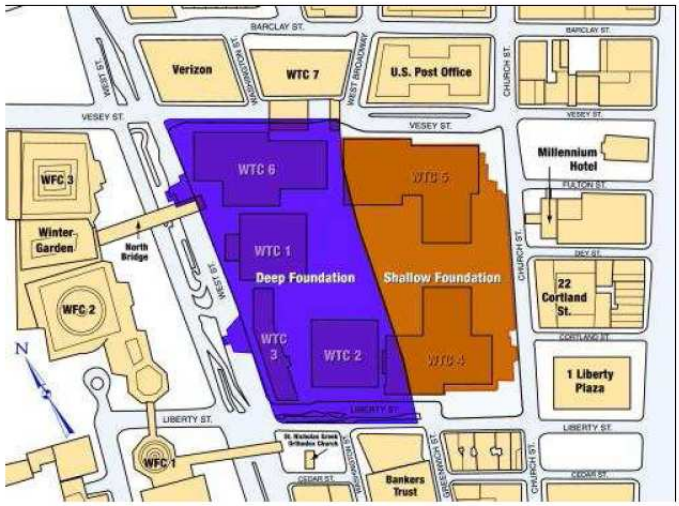

Figure 11. Location of subterranean structure. FEMA report 2000

A deep subterranean structure was present under the WTC Plaza and the two towers. The western half of this substructure, was 70 feet deep and contained six subterranean levels. The structure housed a shopping mall and building mechanical and electrical services, and it also provided a station for the PATH subway line and parking for the complex.

Before the construction, the site was covered by deep deposits of fill material. The perimeter walls for the subterranean structure were constructed using the slurry wall technique. After the concrete wall was cured and attained sufficient strength, excavation of the basement was started. As excavation proceeded downward, tieback anchors were drilled diagonally down through the wall and grouted into position in the rock deep behind the walls. These anchors stabilized the wall against the soil and water pressures from the unexcavated side as the excavation continued on the inside. After the excavation was made, foundations were formed and poured against the exposed bedrock, and the various subgrade levels of the structure were constructed.

Floors within the substructure were of reinforced concrete flat-slab construction, supported by structural steel columns. Many of these steel columns also provided support for the structures located above the plaza level. After the floor slabs were

constructed, they were used to provide lateral support for the perimeter walls, holding back the earth pressure from the unexcavated side. The tiebacks, installed temporarily, were took out by removing their end anchorage and repairing the pockets in the slurry wall where these anchors had existed [1,Chapter2].

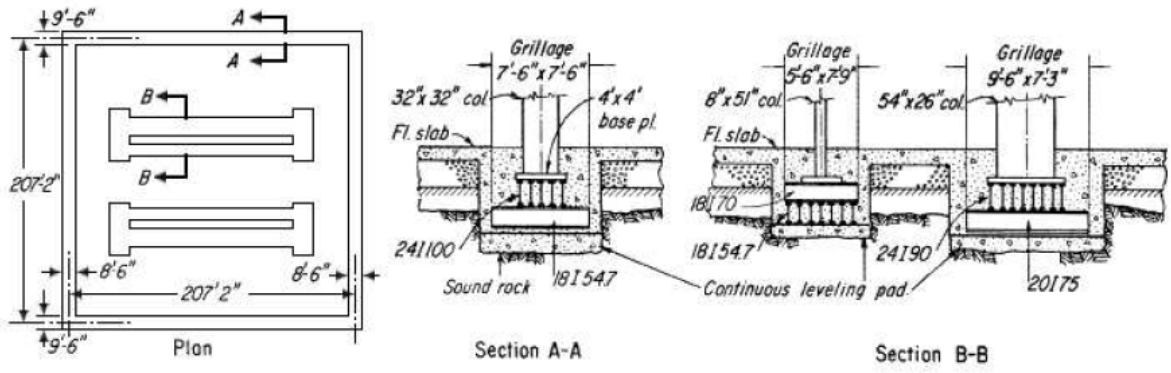

Figure 12. Tower Foudations. FEMA report 2000

Tower foundations beneath the substructure consisted of massive spread footings, bearing directly on the massive bedrock. Steel grillages, consisting of layers of orthogonally placed steel beams, were used to transfer the immense column loads to the reinforced concrete footings [1,Chapter2].

CONSTRUCTION OF THE PERIMETER-WALL FRAME:

The external tube was made of modules consisting of three columns, 3 stories tall, interconnected by spandrel plates. Cap plates were provided at the top and bottom of each column to allow bolted connections with high strength bolt (A365, A490). Connection and strength capacity varied along the building height, with 4 bolt connections at upper stories and 6 bolts connections at lower stories.

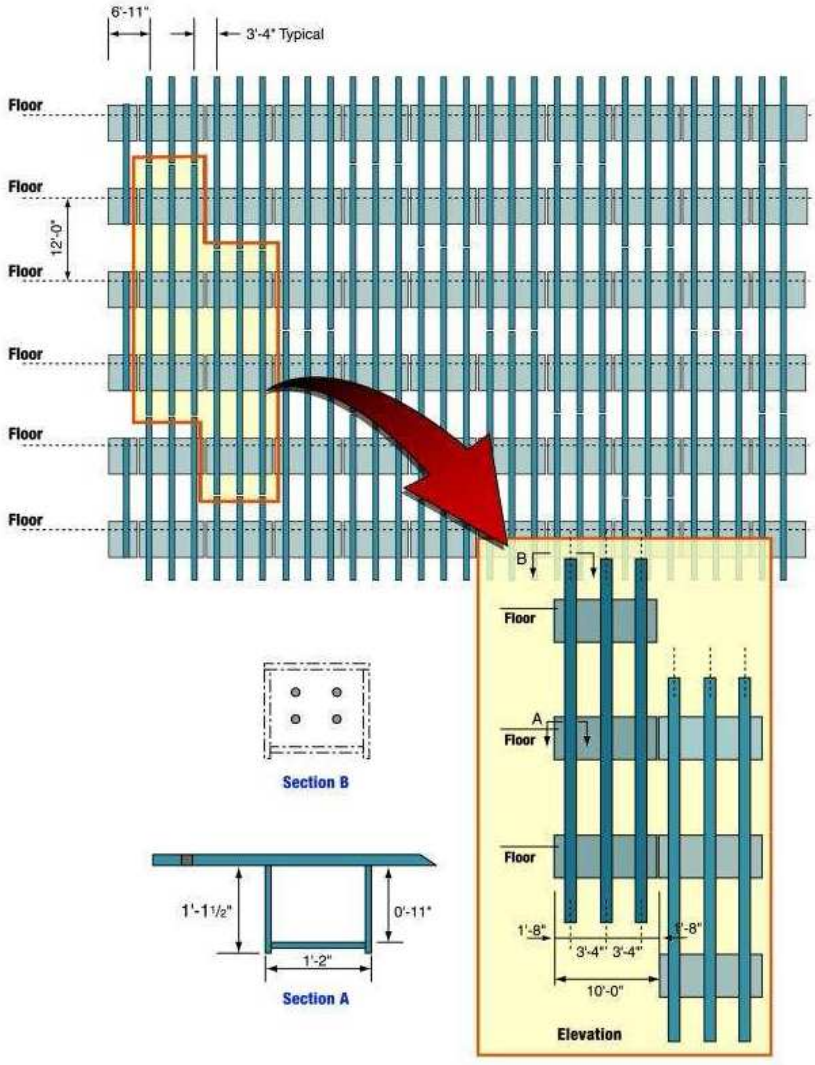

Figure 13. Presents a partial elevation of this exterior wall at typical building floors. FEMA report 2000

The figure above illustrates the construction of typical modules and their interconnection. The construction of the perimeter-wall frame was made of extensive use of prefabricated modules [1,Chapter2]. Each exterior wall module consisted of three columns, three stories tall, interconnected by the spandrel plates, using all-welded construction.

Cap plates were provided at the tops and bottoms of each column, to permit bolted connection to the module above and below. Connection strength varied throughout the building, ranging from four bolts at upper stories to six bolts at lower stories. Near the building base, additional welds were also used.

Side joints of adjacent modules consisted of high-strength bolted shear connections between the spandrels at mid-span. Except at the base of the structures and at mechanical horizontal splices between modules were combined in elevation so that not more than one third of the units were spliced in any one story.

Where the units were all spliced at a common level, additional welds were used to improve the strength of these connections. At the building base, adjacent three columns combined to form a single massive column, in a fork-like formation [1,Chapter 2].

Figure 14. Base of exterior wall frame. FEMA report 2002. FEMA report 2000

Twelve grades of steel, having yield strengths varying between 42 kips (289 MPa) per square inch (ksi, kilopound per square inch) and 100 ksi (689 MPa), were used to fabricate the perimeter column and spandrel plates. Plate thickness also varied both vertically and around the building perimeter, to distribute the predicted loads and minimize differential shortening of columns across the floor plate. In upper stories of the building, plate thickness in the exterior wall was generally 1/4 inch. At the base of the building, column plates were 4 inches thick. The grade and thickness was neither exactly symmetrical within the two towers.

The stiffness of the spandrel plates, created by the combined effects of the short spans and significant depth created a structural system that was stiff both laterally and vertically. Under the effects of lateral wind loading, the buildings essentially behaved as cantilevered hollow structural tubes with perforated walls[1,Chapter 2].

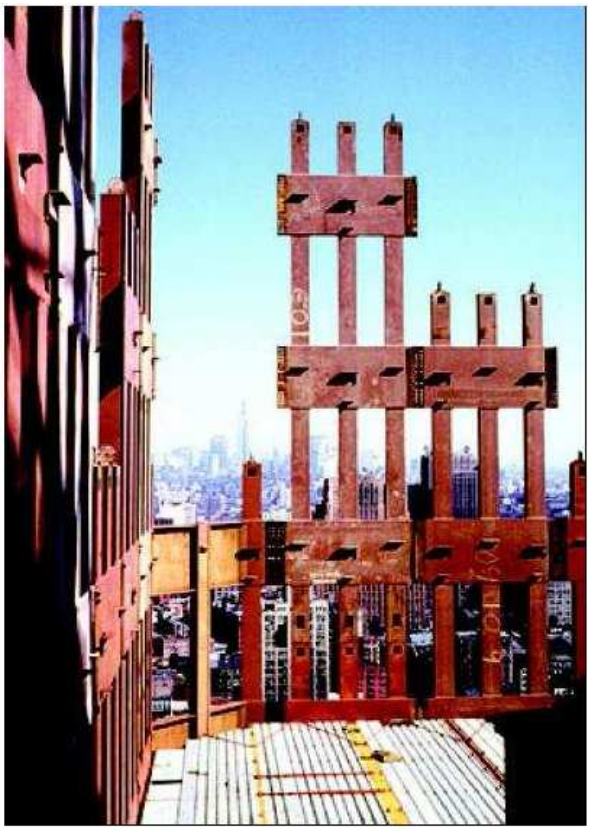

Figure 15. The erection of the prefabricated components, forming the exterior wall and floor deck units. FEMA report 2000

This is the perimeter wall and the steel decking on which the concrete floor slab is poured. The top chords of the trusses (yellow) and the diagonal bars (the V-shaped features) and the rows of shear studs run perpendicular to the main trusses.

Figure 16. The erection of floor framing during original construction. FEMA report 2000

These are the mechanical floors, the only floors for which the prefabricated perimeter wall units were not staggered. The mechanical floors where not supported by trusses but by solid steel beams. Composite action between these beams and the concrete slab was by welded shear studs[1,Chapter2]. The concrete slab was apparently considerably thick and specially reinforced with steel beams. Such floors were necessary to enable the towers to resist the significant lateral force of hurricane force winds.

On the 41st and 42nd floors, both towers housed mechanical equipment. To sustain the heavy loads, the floors were designed as structural steel frame slabs. All other floors from the ninth to the top, except for 75 and 76, which will also carry mechanical equipment, had typical truss floor joists and steel decking.

The office floors had 4-in (10.2 cm) thick slabs of composite construction using top chord knuckles of the trusses, which extended into the slab, as shear connectors. On mechanical floors, composite action was provided by welded stud shear connectors.

The perimeter wall was composed by orthotropic panels with different axial and bending stiffnesses in the horizontal and vertical directions. At the end, the perimeter wall, lost the lateral support of the floors, acting as bracing for the external wall, buckled maybe aided by weaker connections between the panels. In this work I study the buckling of one face of the Towers. To represent only one face of the building I considered the external edges of the structure simply supported but I didn’t put much attention on it because I was interested in the weaker connections between the panels as a possible cause of the collapse. Particularly I examined the extreme case of weak connections using pin connections.

Chapter 2 The Collapse

On the morning of September 11, 2001, two hijacked commercial jetliners were flown into the WTC towers. The first plane, American Airlines Flight 11, originated at Boston's Logan International Airport at 7:59 a.m.. The plane crashed into the north face of the north tower, WTC 1, at 8:46 a.m. The second plane, United Airlines Flight 175, departed Boston at 8:14 a.m. crashed into the south face of the south tower, WTC 2, at 9:03 a.m. Both flights, scheduled to arrive in Los Angeles, were Boeing 767-200ER series aircraft loaded with sufficient fuel for the transcontinental flights [1,Chapter1].

The north tower was struck between floors 94 and 98, with the impact centered on the north face. The south tower was hit between floors 78 and 84 toward the east side of the south face. Each plane caused damage across multiple floors. The speed of impact into the north tower was estimated to be 410 knots,470 miles per hour (mph), and the speed of impact into the south tower was estimated to be 510 knots, 590 mph. As the two aircraft impacted the buildings, fireballs erupted and jet fuel spread across the impact floors igniting fires. The term fireball is used to describe deflagration, or ignition, of a fuel vapor cloud. The fires spread throughout the upper floors of the two WTC towers, thousands attempted to evacuate the buildings. At 9:59 a.m., 56 minutes after it was struck, the south tower collapsed. The north tower continued to stand until 10:29 a.m., when it, too, collapsed. The north tower had survived 1 hour and 43 minutes from the time the jetliner crashed into it [1,Chapter1].

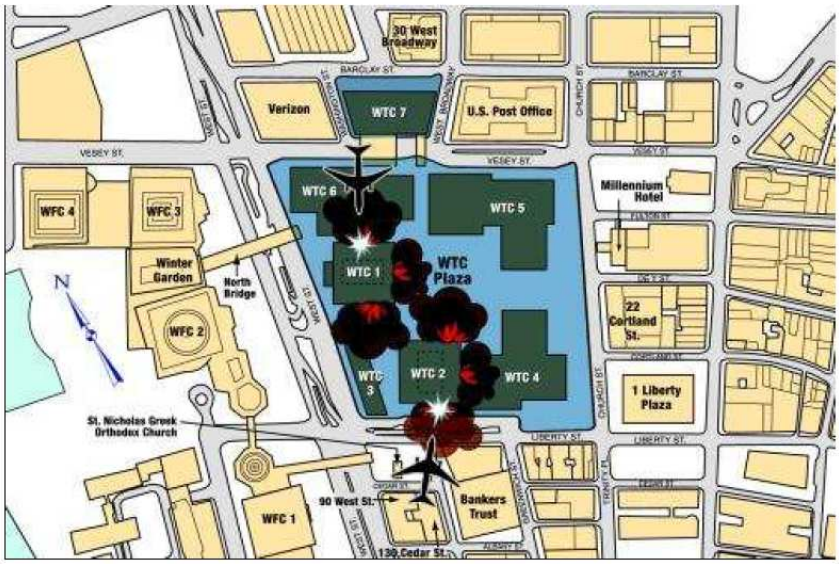

Figure 17. FEMA report 2000

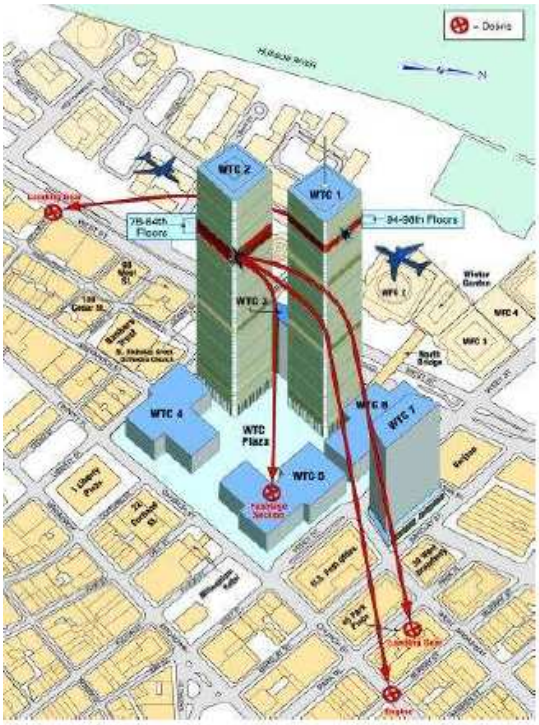

Figure 18. FEMA report 2000

Debris from the collapsing towers fell down on surrounding buildings, causing structural damage and starting new fires. The sudden collapse of each tower sent out air pressure waves that spread dust clouds of building materials in all directions for many blocks. Portions of WTC 3 were severely damaged by debris from each tower collapse, but progressive collapse of the building did not occur[1,Chapter1]. However, little of WTC 3 remained standing after the collapse of WTC 1. WTC 4, 5, and 6 had floor contents and furnishings burn completely and suffered significant partial collapses from debris impacts and from fire damage to their structural frames. WTC 7, a 47-story burned for 7 hours before collapsing at 5:20 p.m.

The building's structural system, composed of the exterior load bearing frame, the gravity load bearing frame at the central core, and the system of deep outrigger trusses in upper stories, was highly redundant. This permitted the building to limit the immediate zone of collapse to the area where several stories of exterior columns were destroyed by the initial impact and, perhaps, to portions of the central core [1,Chapter1]. Following the impact, floor loads originally supported by the exterior columns in compression were successfully transferred to other load paths. Most of the load supported by the failed columns was transferred to adjacent perimeter columns through Vierendeel behavior of the exterior wall frame.

The extra vertical load on the perimeter columns would have been distributed around the whole perimeter frame and would not have been concentrated mainly on adjacent columns. The columns on the impact side would have been in greater compression and the columns on the opposite side would have been in greater tension. The columns on the other two sides would vary from greater compression to greater tension. This is Vierendeel behavior and this is what enabled the towers to resist the lateral force of the wind. The towers were designed to distribute extra loading in this way [1,Chapter1].

The loss of the columns resulted in some immediate tilting of the structure toward the impact area subjecting the remaining columns and the structure to additional stresses from P-delta effects. Also, exterior columns above the zone of impact were converted from compression members to hanger-type tension members, so that, in effect, a portion of the floors' weight became suspended from the outrigger trusses and were transferred back to the interior core columns. The outrigger trusses also would have been capable of transferring some of the load carried by damaged core columns to adjacent core columns.

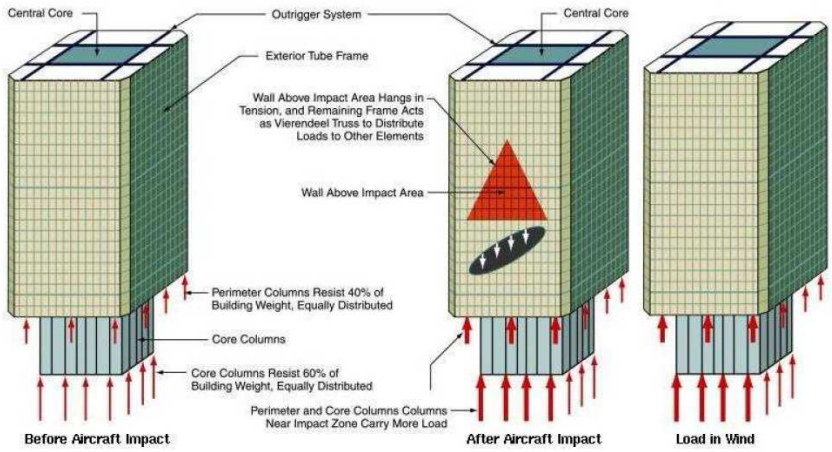

Figure 19. Redistribution of load after aircraft impact and in wind. FEMA report 2000

The primary load path for the redistribution of the load from missing perimeter columns, was through the deep spandrel plates to all the remaining perimeter columns. The World Trade Center towers were specifically designed to spread the load to all the remaining perimeter columns, through both compression and tension. The primary load path for the redistribution of the load from missing core columns, was through the cores rigid three dimensional grid of beams and columns, to all the remaining core columns.

Following the aircraft impact into the building, the structure was able to redistribute the building weight to the remaining elements and to maintain a stable condition for 1 hour and 43 minutes following the impact. However, the structure's global strength was severely degraded. Although the structure may have been able to remain standing in this weakened condition for an indefinite period, it had limited ability to resist additional loading and could potentially have collapsed as a result of any severe loading event, such as that produced by high winds or earthquakes. WTC 1 probably experienced some additional loading and damage due to the collapse of the adjacent WTC 2. This additional damage was not sufficient to cause collapse. The first event of sufficient severity to cause collapse was the fires that followed the aircraft impact [1,Chapter2].

2.1 Structural response to fire loading

The impact of the aircraft into WTC 1 degraded the strength of the structure to withstand additional loading and made the building more susceptible to fire-induced failure. Among the most significant factors:

1- The force of the impact and the debris and fireballs probably compromised the applied fire protection of some steel members in the immediate area of impact. The exact extent of this damage will probably never be known, but this likely resulted in greater susceptibility of the structure to fire-related failure.
2- Some of the columns were under elevated states of stress following the impact, due to the transfer of load from the destroyed and damaged elements.
3- Some portions of floor framing directly beneath the partially collapsed areas were carrying substantial additional weight from the resulting debris and were carrying greater loads than they were designed to resist. As fire spread and increased the temperature of structural members, the structure was further stressed and weakened, until it was unable to support its big weight. Although the specific chain of events that led to the eventual collapse will probably never be identified the following effects of fire on structures may each have contributed to the collapse in some way.
4- As floor framing and supported slabs above and in a fire area are heated, they expand. The towers were designed to survive much more serious fires than those that occurred on September 11. Their design was actually put to the test on

February 23 1975 when the fire occurred in the WTC North Tower. The North Tower suffered no serious structural damage from this intense fire. As a structure expands, it can develop additional, potentially large, stresses in some elements. If the resulting stress state exceeds the capacity of some members or their connections, this can initiate a series of failures.

Concrete takes a long time to heat up, and usually remains relatively cool until the fire has burnt through an area. In intense fires of long duration, the concrete slabs maximum average temperature is usually a few hundred degrees less than that of the steel [1,Chapter 2].

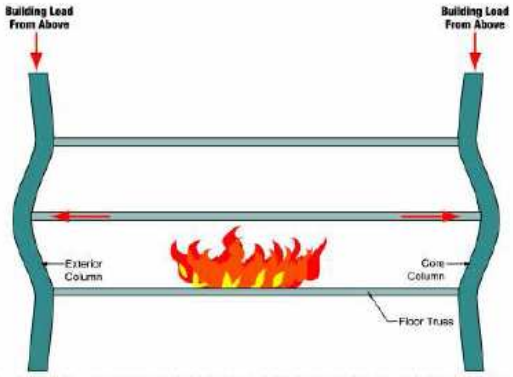

Figure 20. Expansion of floor slabs and framing results in outward deflection of columns and potential overload. FEMA report 2000

In figure above seems that the fire caused the steel to expand and push the exterior walls out, however in figure below the fire caused the steel to sag and pull the exterior walls inward. This was explained saying that at relatively low temperatures the beams/trusses expand axially until they buckle. Once they buckle the thermal expansion is accommodated by sagging. This buckling of the beams/trusses allows the thermal expansion to be accommodated by sagging. The large axial restraint due to the trusses composite action with the concrete and the restraint due to the end columns, means that sagging was the predominant feature. At 500°C, a temperature that the slab probably never reached, the 60 foot sections of concrete floor slab between the core and perimeter wall would expand by about 3 inches, however, this extra length was easily accommodated by the sagging of the slab.

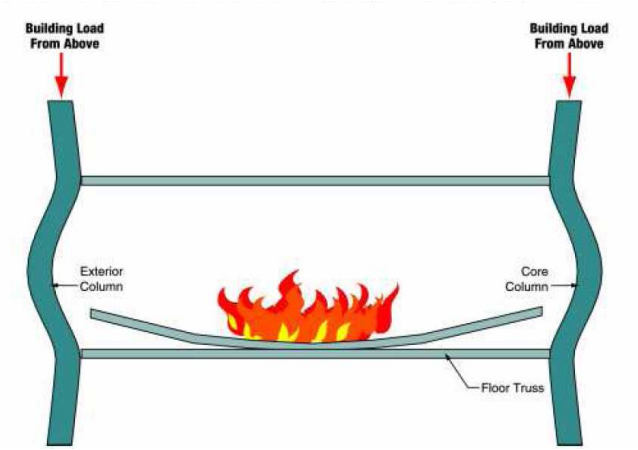

Figure 21 Buckling of columns initiated by failure of floor framing and connections. FEMA report 2000

In the figure below is shown that as the temperature of floor slabs and support framing increases, these elements can lose rigidity and sag into catenary action. As catenary action progresses, horizontal framing elements and floor slabs become tensile elements, which can cause failure of end connections, and allow supported floors to collapse onto the floors below. The presence of large amounts of debris on some floors of WTC 1 would have made them even more sensible to this behavior.

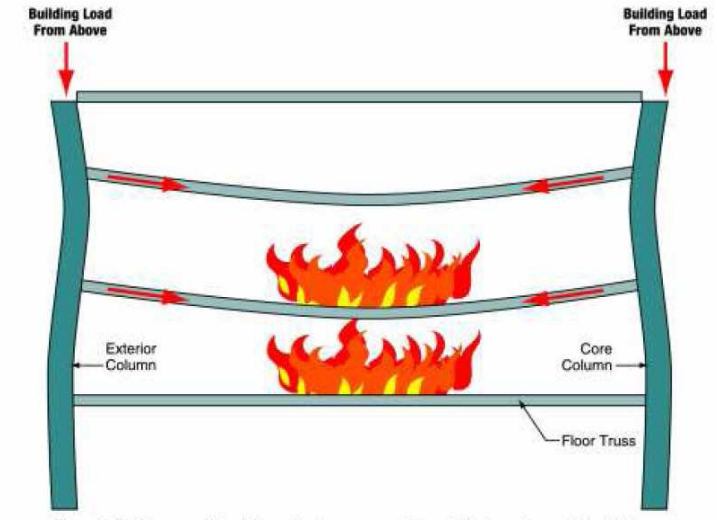

Figure 22. Catenary action of floors framing on several floors initiates column buckling failures. FEMA report 2000

To study deeply if the thermal expansion of the beams /trusses was due to the axial expansion or by sagging, was performed a test at Cardington in which was demonstrated that the thermal expansion was accommodated by downward deflection and not by the forcing of the exterior walls away from the core, axial expansion [1,Chapter2].

Figure 23. Test fire at Cardington FEMA report 2000

There was also no failure of the end connections. Even though the beams could only contribute as catenary tension members (the beams were reduced to 3 or 4% of their room temperature strength), the concrete floors supplied strength to the structural system by membrane action and no collapse occurred. The beams/trusses were not fire protected.

2.2 Progression of the collapse in the WTC 1 and WTC 2

In the construction of WTC 1 and WTC 2 there was stored more than 4×10^{11} joules of potential energy over the 1,368-foot height of the structure. Of this, 8×10^{9} joules of potential energy were stored in the upper part of the structure, above the impact floors, relative to the lowest point of impact. Once collapse initiated, much of this potential energy was rapidly converted into kinetic energy. As the large mass of the collapsing floors above accelerated and impacted on the floors below, it caused an immediate progressive series of floor failures, punching each in turn onto the floor below, accelerating as the sequence progressed.

As the floors collapsed, this left tall freestanding portions of the exterior wall and possibly central core columns. As the unsupported height of these freestanding exterior wall elements increased, they buckled at the bolted column splice connections, and also collapsed. Perimeter walls of the building seem to have come off and fallen directly away from the building face, while portions of the core fell in a somewhat random manner. The perimeter walls broke apart at the bolted connections, allowing individual prefabricated units that formed the wall to fall to the street and onto neighboring buildings below [1, Chapter1].

These studies suggest that the perimeter wall of the tube lost lateral support and buckled, maybe aided by weaker connections between panels. I focus my attention to study the buckling of one face of the external tube to see how it collapses.

Chapter 3 Buckling basic theories

3.1 Thin plates

Thin plates are flat structural members bounded by two parallel planes, called faces, and a cylindrical surface, called an edge or boundary. The distance between the plane faces is the thickness (h) of the plate. It will be assumed that the plate thickness is small compared with other characteristic dimensions of the faces (length, width, diameter,..).

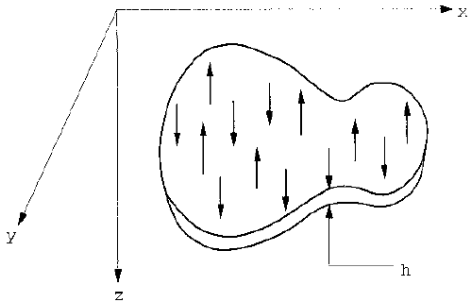

Figure 24 Thin plates and shells-Theory, analysis and applications. Edward Ventsel, Theodor Krauthammer. 2001 Marcel Dekker, Inc. Part I: Thin plates

The loads carried by the plates are predominantly perpendicular to the plate faces.
The load-carrying action of a plate is similar to that of beams or cables and it can be approximated by a gridwork of an infinite number of beams or by a network of an infinite number of cables, depending on the flexural rigidity of the structures [2].

3.2 General Behavior of plates

The plate bending theory based on the Kirchhoff's hypotheses is referred to as the Kirchhoff's plate theory.

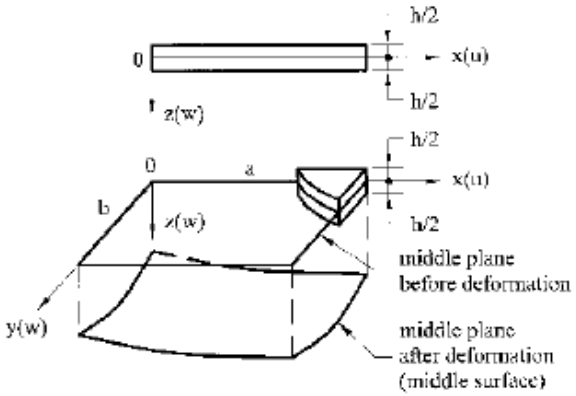

Figure 25. Thin plates and shells-Theory, analysis and applications. Edward Ventsel, Theodor Krauthammer. 2001 Marcel Dekker, Inc. Part I: Thin plates

The fundamental assumptions of the linear, elastic, small-deflection theory of bending for thin plates are the following [2]:

1. The material of the plate is elastic, homogeneous, and isotropic.
2. The plate is initially flat.
3. The deflection (the normal component of the displacement vector) of the midplane is small compared with the thickness of the plate.
4. The straight lines, initially normal to the middle plane before bending, remain straight and normal to the middle surface during the deformation, and the length of such elements is not altered. The vertical shear strains γ_{xz} and γ_{yz} are negligible and the normal strain ε_z may also be omitted. This assumption is referred to as the ''hypothesis of straight normal.''
5. The stress normal to the middle plane, σ_z, is small compared with the other stress components and may be neglected in the stress–strain relations.
6. Since the displacements of a plate are small, it is assumed that the middle surface remains unstrained after bending.

These assumptions result in the reduction of a three-dimensional plate problem to a two-dimensional one.

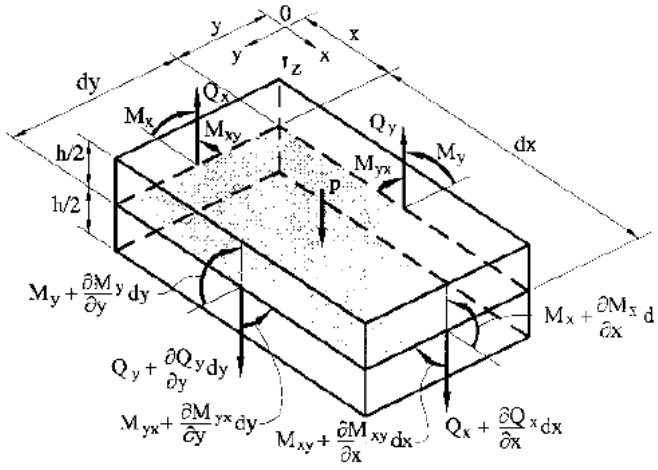

Figure 26. Thin plates and shells-Theory, analysis and applications. Edward Ventsel, Theodor Krauthammer. 2001 Marcel Dekker, Inc. Part I: Thin plates

a. Governing equation for deflection of plates

The components of stress generally vary from point to point in a loaded plate. These variations are governed by the static conditions of equilibrium [2]. Considering a very small element dx x dy of the plate subjected to a vertical distributed load of intensity p(x,y) applied to an upper surface of the plate, the force and moment components may be considered to be distributed uniformly over the midplane of the plate element.
The following three independent conditions of equilibrium may be set up:

1- The force summation in the z axis gives:

$$\frac{\partial Q_x}{\partial x}\mathrm{d}x\mathrm{d}y + \frac{\partial Q_y}{\partial y}\mathrm{d}x\mathrm{d}y + p\mathrm{d}x\mathrm{d}y = 0,$$

from which

$$\frac{\partial Q_x}{\partial x} + \frac{\partial Q_y}{\partial y} + p = 0.$$

2- The moment summation about the x axis leads to

$$\frac{\partial M_{xy}}{\partial x}\mathrm{d}x\mathrm{d}y + \frac{\partial M_y}{\partial y}\mathrm{d}x\mathrm{d}y - Q_y\mathrm{d}x\mathrm{d}y = 0$$

or

$$\frac{\partial M_{xy}}{\partial x} + \frac{\partial M_y}{\partial y} - Q_y = 0.$$

3- The moment summation about the y axis results in

$$\frac{\partial M_{yx}}{\partial y} + \frac{\partial M_x}{\partial x} - Q_x = 0.$$

$$Q_x = \frac{\partial M_x}{\partial x} + \frac{\partial M_{xy}}{\partial y}$$

$$Q_y = \frac{\partial M_{xy}}{\partial x} + \frac{\partial M_y}{\partial y}$$

Taking into account $M_{yx} = M_{xy}$

It is obtained:

$$\frac{\partial^2 M_x}{\partial x^2} + 2\frac{\partial^2 M_{xy}}{\partial x \partial y} + \frac{\partial^2 M_y}{\partial y^2} = -p(x, y).$$

Substituting in it the expression of M_x, M_y, M_{xy} follows the governing equation for the deflections of thin plates bending analysis based on Kirchhoff's assumptions.

$$\frac{\partial^4 w}{\partial x^4} + 2\frac{\partial^4 w}{\partial x^2 \partial y^2} + \frac{\partial^4 w}{\partial y^4} = \frac{p}{D}.$$

This equation was obtained by Lagrange in 1811. Mathematically, the differential equation can be classified as a linear partial differential equation of the fourth order having constant coefficients.

Once a deflection function w(x,y) has been determined, the stress resultants and the stresses can be evaluated. In order to determine the deflection function, it is required to integrate it with the constants of integration dependent upon the appropriate boundary conditions.

The expressions for the vertical forces Qx and Qy, may now be written in terms of the deflection w:

$$Q_x = -D\frac{\partial}{\partial x}\left(\frac{\partial^2 w}{\partial x^2} + \frac{\partial^2 w}{\partial y^2}\right) = -D\frac{\partial}{\partial x}(\nabla^2 w),$$

$$Q_y = -D\frac{\partial}{\partial y}\left(\frac{\partial^2 w}{\partial x^2} + \frac{\partial^2 w}{\partial y^2}\right) = -D\frac{\partial}{\partial y}(\nabla^2 w).$$

b. Boundary conditions

The boundary conditions are the conditions on the surfaces of the plate which must be prescribed in advance in order to obtain the solution of the deflection equation corresponding to the particular problem [2].

1- Clamped edge

At the clamped edge y =0 the deflection and slope are zero:

$$w = 0|_{y=0} \quad \text{and} \quad \vartheta_y \equiv \frac{\partial w}{\partial y} = 0\Big|_{y=0}.$$

2- Simply supported edge

Deflection and bending moment are zero:

$$w = 0|_{x=a},\ M_x = -D\left(\frac{\partial^2 w}{\partial x^2} + \nu\frac{\partial^2 w}{\partial y^2}\right) = 0\Big|_{x=a}.$$

The first of these equations implies that along the edge x=a all the derivatives of w with respect to y are zero, if x = a and w=0, then

$$\frac{\partial w}{\partial y} = \frac{\partial^2 w}{\partial y^2} = 0$$

It follows

$$w = 0|_{x=a},\ \frac{\partial^2 w}{\partial x^2} = 0\Big|_{x=a}.$$

3- Free edge

Bending moment and shear forces are zero

$$M_y = 0\big|_{y=b},\ Q_y = 0\big|_{y=b},\ M_{yx} = 0\big|_{y=b}$$

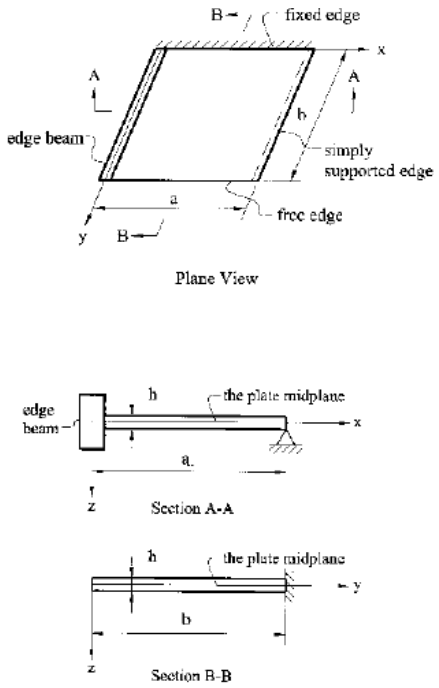

Figure 27. Thin plates and shells-Theory, analysis and applications. Edward Ventsel, Theodor Krauthammer. 2001 Marcel Dekker, Inc. Part I: Thin plates

3.3 Rectangular plates

These plates represent a good model for development and as a check of various methods for solving the governing differential equation. I will consider the solutions in the form of double trigonometric series applied to rectangular simply supported and continuous plates. I will explain two methods to find the solutions of rectangular plates: one, the Navier's method which find the solution in the form of double trigonometric series. Then I will study the buckling of simply supported rectangular plates and to solve it I used software: SAP2000.

I started to study in Sap2000 a rectangular plate simply supported subjected to a uniform load p(x,y) in order to see how is it the buckling behavior of a plate and after I built a simplified model of one face of the World Trade Center to study the collapse. The complicate thing of this design is the reproduction of the connection between the panels. When I started I thought that the main problem of the collapse was in the kind of connection between the panels. To see this peculiar aspect I studied 2 different kinds of plates: one with continuous panels and one with hinged panels as the extreme case. At the end of the experimentations performed I saw that the buckling in the two cases isn't so different. At the beginning I expected that the plate with the hinged panels would buckle faster than the continuous plate, after getting off one, 1, 2, 3, 4 floors. In reality I

got almost the same buckling in the two cases. I will explain later in more detail this aspect, now I want to introduce the behavior of the rectangular plate and the buckling of the plates. After I will show the models that I built.

Navier's method

Navier found the solution of bending of simply supported plates by double trigonometric series [2]. The boundary conditions for a simply supported rectangular plate subjected to a uniform load p(x,y) are:

$$w = 0|_{x=0,a};\ \frac{\partial^2 w}{\partial x^2} = 0\Big|_{x=0,a} \quad \text{and} \quad w = 0|_{y=0,b};\ \frac{\partial^2 w}{\partial y^2} = 0\Big|_{y=0,b}.$$

The solution of the governing differential equation is:

$$\frac{\partial^4 w}{\partial x^4} + 2\frac{\partial^4 w}{\partial x^2 \partial y^2} + \frac{\partial^4 w}{\partial y^4} = \frac{p}{D}.$$

The expressions of the deflection surface, w(x,y), and the distributed surface load, p(x,y), have to be sought in the form of an infinite Fourier series, as follows:

$$w(x,y) = \sum_{m=1}^{\infty}\sum_{n-1}^{\infty} w_{mn} \sin\frac{m\pi x}{a}\sin\frac{n\pi y}{b},$$

$$p(x,y) = \sum_{m=1}^{\infty}\sum_{n-1}^{\infty} p_{mn} \sin\frac{m\pi x}{a}\sin\frac{n\pi y}{b},$$

where w_{mn} and p_{mn} represent coefficients to be determined. It can be easily verified that the expression for deflections satisfies the prescribed boundary conditions.

To determine the Fourier coefficients p_{mn}, each side of the distributed load equation is multiplied by sin lπx/a sin kπy/b and integrated twice between the limits 0,a and 0,b, as follows:

$$\int_0^a\int_0^b p(x,y)\sin\frac{l\pi x}{a}\sin\frac{k\pi y}{b}\,dx\,dy =$$

$$\sum_{m=1}^{\infty}\sum_{n=1}^{\infty} p_{mn}\int_0^a\int_0^b \sin\frac{m\pi x}{a}\sin\frac{n\pi y}{b}\sin\frac{l\pi x}{a}\sin\frac{k\pi y}{b}\,dx\,dy.$$

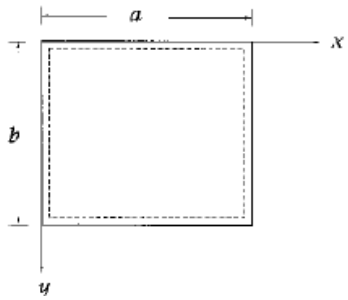

Figure 28. Thin plates and shells-Theory, analysis and applications. Edward Ventsel, Theodor Krauthammer. 2001 Marcel Dekker, Inc. Part I: Thin plates

It can be shown by direct integration that

$$\int_0^a \sin\frac{m\pi x}{a}\sin\frac{l\pi x}{a}dx = \begin{cases} 0 \text{ if} m \neq l \\ a/2 \text{ if } m = l \end{cases}$$

$$\text{and } \int_0^b \sin\frac{n\pi y}{b}\sin\frac{k\pi y}{b}dy = \begin{cases} 0 \text{ if } n \neq k \\ b/2 \text{ if } n = k. \end{cases} +$$

The coefficients of the double Fourier expansion are the following:

$$p_{mn} = \frac{4}{ab}\int_0^a\int_0^b p(x,y)\sin\frac{m\pi x}{a}\sin\frac{n\pi y}{b}dxdy.$$

$$p_{mn} = \frac{4}{ab}\int_0^a\int_0^b p(x,y)\sin\frac{m\pi x}{a}\sin\frac{n\pi y}{b}dxdy.$$

Since the representation of the deflection satisfies the boundary conditions, then the coefficients wmn must satisfy the governing differential equation. Substituting the w(x,y) equation into the differential equation results in the following equation:

$$\sum_{m=1}^{\infty}\sum_{n=1}^{\infty}\left\{w_{mn}\left[\left(\frac{m\pi}{a}\right)^4 + 2\left(\frac{m\pi}{a}\right)^2\left(\frac{n\pi}{b}\right)^2 + \left(\frac{n\pi}{b}\right)^4\right] - \frac{p_{mn}}{D}\right\}\sin\frac{m\pi x}{a}\sin\frac{n\pi y}{b} = 0.$$

This equation must apply for all values of x and y. We conclude that

$$w_{mn}\pi^4\left(\frac{m^2}{a^2} + \frac{n^2}{b^2}\right)^2 - \frac{p_{mn}}{D} = 0,$$

from which

$$w_{mn} = \frac{1}{\pi^4 D}\frac{p_{mn}}{\left[(m/a)^2 + (n/b)^2\right]^2}.$$

Substituting the above into w(x,y) equation, one obtains the equation of the deflected surface, as follows:

$$w(x,y) = \frac{1}{\pi^4 D}\sum_{m=1}^{\infty}\sum_{n=1}^{\infty}\frac{p_{mn}}{\left[(m/a)^2 + (n/b)^2\right]^2}\sin\frac{m\pi x}{a}\sin\frac{n\pi y}{b},$$

It can be shown, by noting that $|\sin m\pi x/a| \leq 1$ and $|\sin n\pi y/b| \leq 1$ for every x and y and for every m and n, that the series is convergent.

Substituting w(x,y) we can find the bending moments and the shear forces in the plate, and then determine the stress components.

$$M_x = \frac{1}{\pi^2}\sum_{m=1}^{\infty}\sum_{n=1}^{\infty} p_{mn}\frac{[(m/a)^2 + \nu(n/b)^2]}{[(m/a)^2 + (n/b)^2]^2}\sin\frac{m\pi x}{a}\sin\frac{n\pi y}{b},$$

$$M_y = \frac{1}{\pi^2}\sum_{m=1}^{\infty}\sum_{n=1}^{\infty} p_{mn}\frac{[(n/b)^2 + \nu(m/a)^2]}{[(m/a)^2 + (n/b)^2]^2}\sin\frac{m\pi x}{a}\sin\frac{n\pi y}{b},$$

$$M_{xy} = -\frac{1_\nu}{\pi^2}\sum_{m=1}^{\infty}\sum_{n=1}^{\infty} p_{mn}\frac{mn}{ab[(m/a)^2 + (n/b)^2]^2}\cos\frac{m\pi x}{a}\cos\frac{n\pi y}{b}.$$

The infinite series solution for the deflection generally converges quickly; The accuracy can be obtained by considering only a few terms. Since the bending moment and the shear forces are obtained from the second and third derivatives of the deflection w(x,y), the convergence of the infinite series expressions of the internal forces and moments is less rapid, especially in the vicinity of the plate edges. This slow convergence is also accompanied by some loss of accuracy in the process of calculation. The accuracy of solutions and the convergence of series expressions of the bending moment and shear forces can be improved by considering more terms in the expansions and by using a special technique for an improvement of the convergence of Fourier's series.

3.4 Buckling of plates

Buckling or elastic instability of plates is of great importance.

The buckling load depends on the plate thickness: the thinner the plate, the lower is the buckling load. In many cases, a failure of thin plate elements may be attributed to an elastic instability and not to the lack of their strength [2].

a. The theory of stability of plates

The stability analysis of plates is similar to the Euler stability analysis of columns.

Depending on values of the applied in-plane loads, an initial, state of equilibrium may be stable or unstable. The initial configuration of elastic equilibrium is stable, if when the plate is displaced from this equilibrium state by an infinitesimal disturbance, as a small lateral force, the deflected plate will tend to come back to its initial configuration when the disturbance is removed. The initial configuration of equilibrium is said to be unstable if, when the plate is displaced from this equilibrium position by a small lateral

load, it doesn't return to its initial configuration when the load is removed. The unstable plate will find other new equilibrium states, which may be in the vicinity of the initial state or may be far away from the initial equilibrium configuration.
If the plate remains at the displaced position even after the small lateral load is removed, it is said to be in neutral equilibrium; thus, the plate in neutral equilibrium is neither stable nor unstable. The transition of the plate from the stable state of equilibrium to the unstable one is referred to as buckling or structural instability [2].

The smallest value of the load producing buckling is called the critical or buckling load.
The importance of buckling is the beginning of a deflection, which if the loads are increased above their critical values, rapidly leads to very large lateral deflections. Consequently, it leads to large bending stresses, and eventually to complete failure of the plate.
It is important that a plate leading from the stable to unstable configuration of equilibrium always passes through the neutral state of equilibrium, which is the state between the stable and unstable configurations.
Neutral equilibrium is associated with the existence of bifurcation of the deformations. The critical load can be identified with the load corresponding to the bifurcation of the equilibrium states, or the critical load is the smallest load at which both the flat equilibrium configuration of the plate and deflected configuration are possible.
The goal of the buckling analysis of plates is to determine the critical buckling loads and the corresponding buckled configuration of equilibrium [2].

The linear buckling analysis of plates is based on the following assumptions:

1- Prior to loading, a plate is ideally flat and all the applied external loads act in the middle plane of the plate.
2- States of stress is described by equations of the linear plane elasticity. Any changes in the plate dimensions are neglected prior to buckling.
3- All the loads applied to the plate are dead loads; that is, they are not changed either in magnitude or in direction when the plate deforms.
4- The plate bending is described by Kirchhoff's plate bending theory

The linear buckling analysis of plates based on these assumptions makes it possible to determine accurately the critical loads, which are important in the stability analysis of

thin plates. This analysis gives no way of describing the behavior of plates after buckling, which is also of considerable interest.

Buckling problems of plates can be formulated using the equilibrium method, the energy method, and the dynamic method. I focus the attention on the equilibrium method.

b. The equilibrium method of rectangular plates

Considering a plate subjected to the external edge loads acting in the middle plane of the plate, the in-plane stress resultants in the initial state of equilibrium are Nx; Ny; and Nxy. They may be found from the solution of the plane stress problem for the given plate geometry and in-plane external loading.

For the plate, the in-plane external edge loads that result in an elastic instability as in the case of a beam column, are independent of the lateral loads. The governing differential equation of the linear buckling analysis of plates is obtained from the differential equation by making p equal zero [2]. We have the following:

$$\frac{\partial^4 w}{\partial x^4} + 2\frac{\partial^4 w}{\partial x^2 \partial y^2} + \frac{\partial^4 w}{\partial y^4} = \frac{1}{D}\left(N_x \frac{\partial^2 w}{\partial x^2} + 2N_{xy}\frac{\partial^2 w}{\partial x \partial y} + N_y \frac{\partial^2 w}{\partial y^2}\right).$$

Where Nx; Ny; and Nxy are the internal forces acting in the middle surface of the plate due to the applied in-plane loading. The right-hand side can be interpreted as a fictitious transverse load.

The mathematical problem is to solve this equation with appropriate homogeneous boundary conditions. In general, this problem has only a trivial solution corresponding to the initial state of equilibrium (w≠ 0). However, the coefficients of the governing equation depend on the magnitudes of the stress resultants, which are connected with the applied in-plane external forces, and we can find values of these loads for which a nontrivial solution is possible. The smallest value of these loads will correspond to a critical load.

A more general formulation of the equilibrium method transforms the stability problem into an eigenvalue problem. It is multiplied a reference value of the stress resultants (N′x; N′y; and N′xy) by a load parameter λ

$$N_x = -\lambda \bar{N}_x, \quad N_y = -\lambda \bar{N}_y, N_{xy} = -\lambda \bar{N}_{xy}$$

Substituting it, is obtained an alternative form of the governing differential equation of plate buckling problems:

$$\nabla^4 w + \frac{\lambda}{D}\left(\bar{N}_x \frac{\partial^2 w}{\partial x^2} + \bar{N}_y \frac{\partial^2 w}{\partial y^2} + 2\bar{N}_{xy} \frac{\partial^2 w}{\partial x \partial y}\right) = 0.$$

The solution of w(x,y), obtained by the analytical or numerical methods involves arbitrary constant coefficients Ci (i =1, 2, . . , n) to be determined from the prescribed boundary conditions.

So the differential equation is reduced to a system of homogeneous, linear algebraic equations in Ci. For an existence of a nontrivial solution of the system, its determinant must be equal to zero. This results in the characteristic equation in λ.

Solving this characteristic equation, we obtain some specific values λ1, λ2, . . . ,λn (the characteristic numbers or eigenvalues) and the corresponding non zero solutions, called characteristic functions or eigenfunctions. The smallest of the characteristic numbers or eigenvalues not equal to zero will be the critical value, λcr, and the corresponding eigenfunctions will be the buckling modes. Then, the critical load is calculated by multiplying λcr and the corresponding reference value of the load.

$$Pcr = \lambda cr * Pref$$

c. Buckling of rectangular plates

According to the equilibrium method, the critical values of applied in-plane forces may be found from the solution of the governing differential equation which is a homogeneous, linear partial differential equation with variable coefficients. It is impossible to find its analytical solution in the general case [2].. I illustrate the equilibrium method for obtaining the exact solutions associated with determining the critical forces in simply supported rectangular plates

In my work, to become familiar with the plates, I begun to study the critical buckling load for a simply supported plate subjected to a uniformly distributed compressive edge load qx acting in the x direction and I solved it with the software SAP2000, but I want explain the basic theory of this problem.

For this case Nx=qx and Ny=Nxy=0.

The differential equation becomes

$$D\nabla^2\nabla^2 w + N_x \frac{\partial^2 w}{\partial x^2} = 0.$$

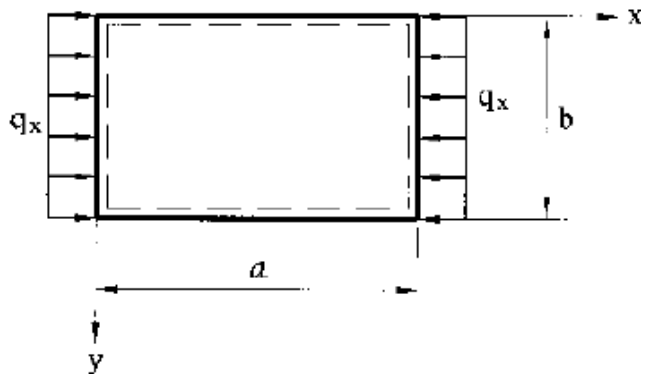

Figure 29. Thin plates and shells-Theory, analysis and applications. Edward Ventsel, Theodor Krauthammer. 2001 Marcel Dekker, Inc. Part I: Thin plates

I seek the solution that satisfies the simply supported boundary conditions. Inserting this solution into this equation

$$\frac{\partial^4 w}{\partial x^4} + 2\frac{\partial^4 w}{\partial x^2 \partial y^2} + \frac{\partial^4 w}{\partial y^4} = \frac{1}{D}\left(N_x \frac{\partial^2 w}{\partial x^2} + 2N_{xy}\frac{\partial^2 w}{\partial x \partial y} + N_y \frac{\partial^2 w}{\partial y^2}\right),$$

leads the following equation.

$$\sum_{m=1}^{\infty}\sum_{n=1}^{\infty}\left[D\pi^4\left(\frac{m^2}{a^2}+\frac{n^2}{b^2}\right)^2 - q_x\pi^2\frac{m^2}{a^2}\right]w_{mn}\sin\frac{m\pi x}{a}\sin\frac{n\pi y}{b} = 0.$$

One possible solution is w_{mn} =0; however, this represents the trivial solution, w(x,y)=0, and corresponds to an equilibrium in the unbuckled, state of the plate and is of no interest. Another possible solution is obtained by setting the quantity in square brackets to zero

$$\pi^4 D\left(\frac{m^2}{a^2}+\frac{n^2}{b^2}\right)^2 - q_x\pi^2\frac{m^2}{a^2} = 0,$$

From which

$$q_x = \frac{\pi^2 D}{b^2}\left(\frac{mb}{a}+\frac{n^2 a}{mb}\right)^2.$$

The constants w_{mn} remain undetermined. This expression gives all values of q_x corresponding to m=1,2,3, ; n=1,2,3, . . . as possible forms of the defected surface. From all of these values one must select the smallest, which will be the critical value. The smallest value of q_x is obtained for n =1. For n=1 qx becomes

$$N_x = \frac{\pi^2 D}{b^2}\left(\frac{mb}{a}+\frac{a}{mb}\right)^2$$

Or

$$q_x = K\frac{\pi^2 D}{b^2},$$

Where K is the buckling load parameter which is defined as:

$$K = \left(\frac{mb}{a}+\frac{a}{mb}\right)^2$$

For a given value of m, the parameter K depends only on the ratio a/b called aspect ratio of the plate. The smallest value of qx and the value of the critical force q_{xcr}, depends on the number half sin waves in the longitudinal direction m. For a given aspect ratio the critical load is obtained by selecting m so that it makes the equation of qx a minimum. Since K depends only on m, we have the following:

$$\frac{dK}{dm} = 2\left(\frac{mb}{a}+\frac{a}{mb}\right)\left(\frac{b}{a}-\frac{a}{m^2 b}\right) = 0.$$

Since the first factor in the parentheses of the above is nonzero, we obtain

$$m = \frac{a}{b}$$

This provides the following minimum values of the critical load

$$Minqx = qxcr = \frac{4\pi^2 D}{b^2}$$

The corresponding value of the buckling load parameter is K=4. The corresponding critical stress is found to be

$$\sigma_{x,cr} = \frac{N_{x,cr}}{h} = \frac{q_{x,cr}}{h} = \frac{4\pi^2 D}{b^2 h} = \frac{\pi^2 E}{3(1-v^2)}\left(\frac{h}{b}\right)^2.$$

The critical values of qx and σx correspond to a plate of a width, b, length, a. The variation of the buckling load parameter K as a function of the aspect ratio a=b for m=1,2,3,4 is shown in the figure below.

The magnitude of qxcr and the number of half-waves m, in the direction of the applied compressive forces, for any value of the aspect ratio can readily be found. If a/b=1,5, K=4,34 and m=2 and The corresponding critical load is

$$q_{x,\mathrm{cr}} = 4.34\frac{\pi^2 D}{b^2}.$$

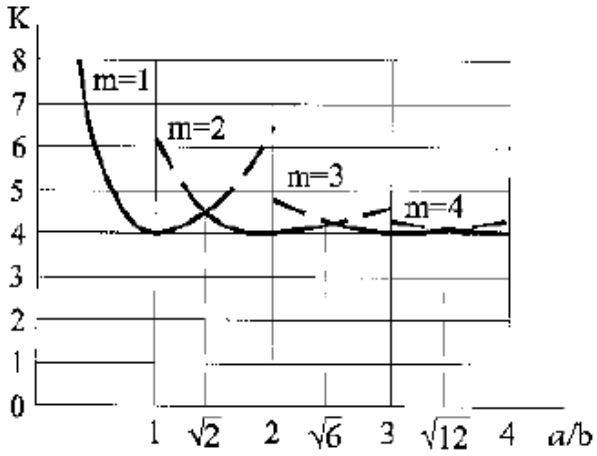

Figure 30. Thin plates and shells-Theory, analysis and applications. Edward Ventsel, Theodor Krauthammer. 2001 Marcel Dekker, Inc. Part I: Thin plates

The plate buckles under this load into two half-waves in the direction of the applied compressive loads and one-half in the perpendicular direction.

Short and broad plates (a/b < 1) a minimum value of the critical force is obtained for m=1. For a/b << 1, that is for very short and broad plates, the ratio a/b can be neglected compared with the ratio b/a and $K \approx b^2/a^2$

The value of the critical force is:

$$q_{x,\mathrm{cr}} = 4.34\frac{\pi^2 D}{b^2}.$$

Thus, in this case, the critical force does not depend on the plate width, depends only upon its length. The above expression represents the Euler critical load for a strip of unit width and of length a, and the smallest value of flexural rigidity, EI, is replaced with the flexural rigidity of the plate, D.

$$D = \frac{Et^3}{12(1-\nu^2)}$$

Chapter 4 Model of the tube collapse

4.1 Finite Element Model

I solved the structure with the Finite element software SAP2000 which allows to perform:

- Static and dynamic analysis
- Linear and nonlinear analysis
- Dynamic seismic analysis and static pushover analysis

I performed a static and linear buckling analysis of one face of the external tube of the Twin Towers.

In this work my goal is to study the structural collapse of the Twin Towers. To study it I focused the attention on one face of the external tube. My model consists of a rectangular plate simply supported on the lateral edges and fixed at the bottom with a live load applied at the top of the plate. I performed the analysis with SAP2000. I started with the linear static analysis and then the linear buckling analysis through the eigenvalue problem.

To study this type of structure I implemented 2 different models with different characteristics to be able to compare the results and to see the different behavior of the collapse if we consider the structure with different conditions. In fact my goal was to see how the collapse changes if we have a structure made with single continuous panels or with single panels but with weak connections represented by hinges.

My work consists of the study of 2 cases of plates:

1- A plate with continuous panels: this case is important because it allowed to compare this one with the model in which the panels are connected with hinges.

2- A plate with hinged panels: this is the case that better represents the actual structure of the Twin Towers. Implementing this model I obtained results that doesn't show a very big difference with the continuous case. Later I will explain more detailed the behavior of this plate.

4.2 Construction of the model

First of all I defined the dimensions of the plate. The dimensions of the plate I studied aren't the actual one of the World Trade Center. The real dimensions of the external tube of the Twin Towers were 63x63 meters wide and 415 meters high. I studied one face of the structure but smaller in order to simplify the calculations and the analysis. The plate I considered has the following measures:

Width= 24m

Height= 120 m

Panels dimensions:
W= 4 m
H=12m
Floors height: 4 meters
Axial stiffness:
Ax/Ay=0.5
Bending stiffness Kx/Ky=0.1

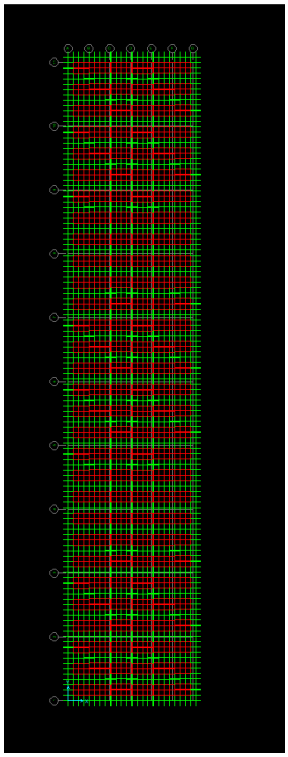

Figure 31. Construction of the model

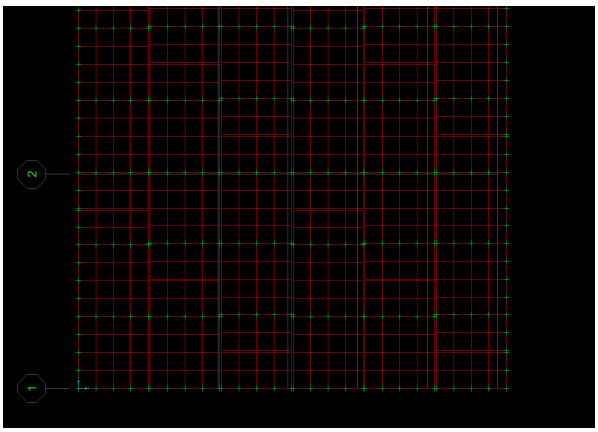

Figure 32. A zoom of the model to see the gap between the panels

I decided these dimensions to simplify the design of the panels. In the x direction I put 6 panels 4 meters wide and in the y direction 10 panels, 12 meters high, respecting the

ratio with the actual structure, in which the panels where 3 meters wide and 11 meters high.

Each panel is 3 stories tall and 4 meters wide, because it includes three columns of 1 meter wide. In my design I didn't built the columns. To take them into considerations I took a different stiffness in the horizontal and vertical directions in terms of bending and axial stiffness. The horizontal axial stiffness is half than the vertical axial stiffness.
The panels are staggered, each one begins in the middle of a floor. The beginning and the end of two near panels doesn't coincide.
After having defined the geometry I chose the material.

Material:

Steel: A992Fy50

E: 199947 Mpa

v: 0.3

Thickness: 0.025m taking into account the ratio t/b=0.006

Width=4m

t/w= 0.025/4=0.00625

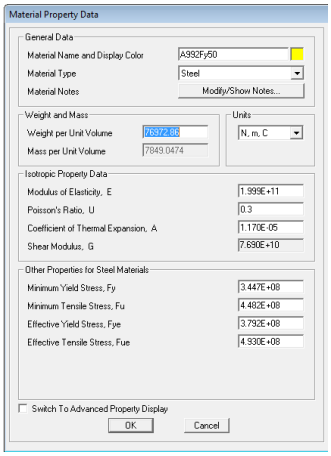

Figure 33 Material property Data.Sap2000

I applied a reference load:

$$Po = \frac{10 \cdot 30}{24.5} = 12.25\ KN/m$$

Then I had to decide the section type of my plate. I chose the shell thin because is more flexible than the thin plate.

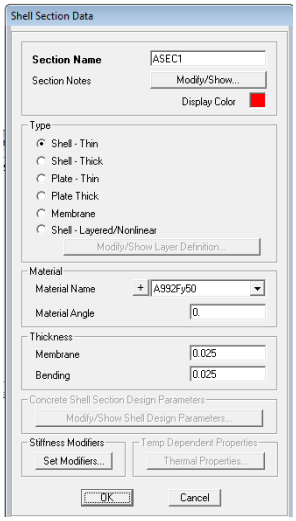

Figure 34 Shell Section Data.Sap2000

Shell elements

I chose the shell element because it is used to model plate behavior in planar and three dimensional structures.

The Shell element is a three- or four-node formulation that combines separate membrane and plate-bending behavior. The four-joint element does not have to be planar [3]. The membrane behavior uses an isoparametric formulation that includes translational in-plane stiffness components and a rotational stiffness component in the direction normal to the plane of the element. The plate bending behavior includes two-way, out-of-plane, plate rotational stiffness components and a translational stiffness component in the direction normal to the plane of the element.

Each Shell element may have a quadrilateral or triangular shape. In my model I used quadrilateral shape because it is more accurate than the triangular one.

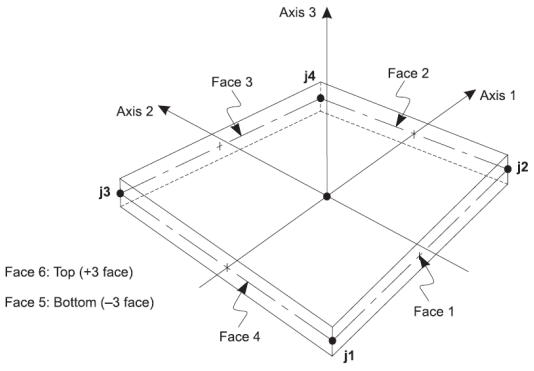

Figure 35. Four node quadrilateral shell element.Sapreference

The difference with the plate element is in the number of degree of freedom in fact the plate has 3 degree of freedom and the shell elements have 6.

The Shell element always activates all six degrees of freedom at each of its connected joints. When the element is used as a pure membrane, it is important to ensure that restraints or other supports are provided to the degrees of freedom for normal translation and bending rotations. When the element is used as a pure plate, it must be ensured that restraints or other supports are provided to the degrees of freedom for in plane translations and the rotation about the normal [3]. In my model I used both membrane and plate behavior because it is recommended for all three-dimensional structures.

Then I decided the boundary conditions and the load. The plate is simply supported in the lateral edges and clamped at the bottom. The difficulties that I faced in my work have been to find the type of connections between the panels. The panels are connected with hinges in the horizontal direction to have the moment release about the x axis, and in the vertical directions they are connected as continuous panels, so the displacements and the rotations are the same in all the directions. Studying the manual I found that for my work the best choice was to apply welds constraints. A weld can be used to connect different parts of the structural model that are defined using separate meshes. A weld is not a single constraint, but a set of joints from which the program automatically generate multiple Body constraints to connect coincident Joints.
Constraints are used to enforce certain types of rigid-body behavior, to connect together different parts of the model, and to impose certain types of symmetry conditions.
Joints are considered to be coincident if the distance between them is less than or equal to a tolerance, **tol**, that has to be specified.
One or more Welds may be defined, each with its own tolerance. Only the joints within each Weld will be checked for coincidence with each other. In the most common case, a single Weld is defined that contains all joints in the model; all coincident groups of joints will be welded [3].

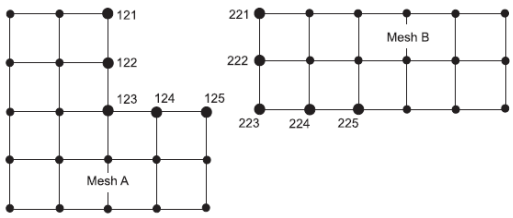

Figure 36. weld constraints. Sapreference

Then I started to compute the analysis and I began with the linear static analysis and then I performed the linear buckling analysis.

Linear static analysis

The static analysis of a structure involves the solution of the system of linear equations represented by:

$$\boldsymbol{K\,u = r}$$

where ***K*** is the stiffness matrix, ***r*** is the vector of applied loads, and ***u*** is the vector of resulting displacements. For each Load Case defined, the program automatically creates the load vector ***r*** and solves for the static displacements ***u***. In my model I set the linear and the buckling load case [3].

Linear buckling analysis through the eigenvalue problem

A linear buckling analysis is an eigenvalue problem and is formulated as follow:

$$([K] + lcr\,[Kg])\{d\} = \{0\}$$

[K] is the stiffness matrix
[lcr] is the eigenvalue for buckling mode
[Kg] is the stress stiffness matrix. This matrix includes the effects of the membrane loads on the stiffness of the structure. The stress stiffening matrix is assembled based on the results of a previous linear static analysis
[d] is the displacement vector corresponding to the buckling mode shape

The eigenvalue solution uses an iterative algorithm that extracts firstly the eigenvalues λcr and after the displacements that define the corresponding mode shape. One set of these is extracted for each of the buckling modes of the structure. The displacements given by the solution aren't real displacements.

λcr= buckling load/applied load

The eigenvalue is a safety factor against buckling. An eigenvalue less than 1 indicates that a structure has buckled under the applied load. An eigenvalue greater than 1 indicates that a structure will not buckle.
Only the membrane component of the loads in the structure is used to determine the buckling load, since the formulation of KG is based only on the membrane loads. This means that the effect of the prebuckling rotations due to moments is ignored [5].

4.3 Case 1: Plate with continuous panels

I started with the continuous case. First I decided the dimensions and the material of the plate.

Width= 24m

Height= 120m

6 panels in the horizontal direction

10 panels in the vertical direction

Reference load:

$$Po = 12.25\ KN/m$$

Joints Restraints

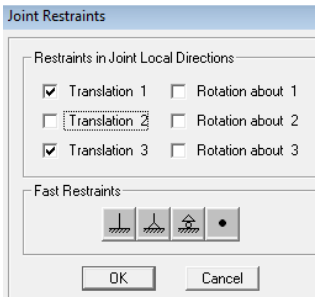

Figure 37. Joints restraints

On the top:	On the right side:	On the bottom I fixed it:
Ux=0	Uz=0	Ux=0
Uz=0		Uy=0
		Uz=0

I chose the thickness following this ratio: t/w=0.006 according to the real dimensions of the Twin Towers in which the ratio was: 63/0.4=0.006

Consequently if w is the width of my plate and measures 24m because is formed by 6 panels of 4 meters wide, the thickness I took is of: 0.025m

At this point I introduced the connections between the panels. As I mentioned before I used weld connections which allow having the same displacements and rotation between two coincident joints of two separate meshes. Below I reported a sketch of the panels in which it is shown the gap between the panels. The gap is of 0.1m and I put a tolerance of 0.2m. The conditions of the constraints are the same in the both directions.

Ux1=Ux2	Rx1=Rx2
Uy1=Uy2	Ry1=Ry2
Uz1=Uz2	Rz1=Rz2

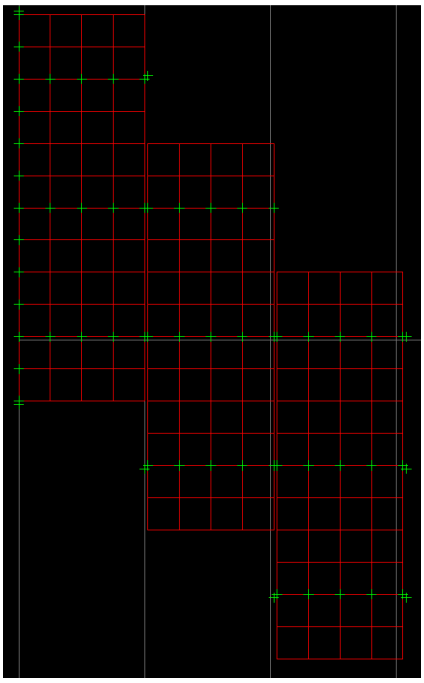

Figure 62. Panels detail

In this case the buckling capacity is Pc.

λcr= 13.8

$$Pc = 13.8 \cdot 12.25 = 169\ KN/m$$

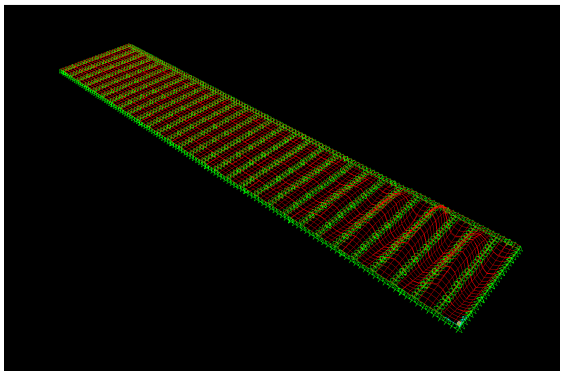

Figure 63. Buckling mode shape

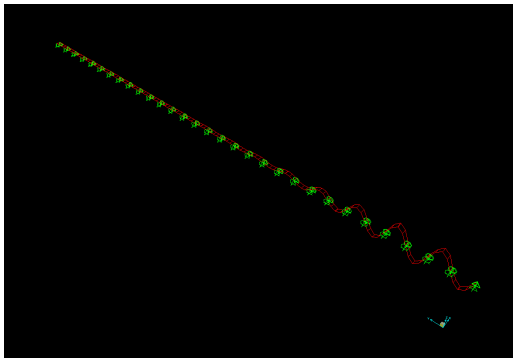

Figure 64. Line selection buckling mode shape

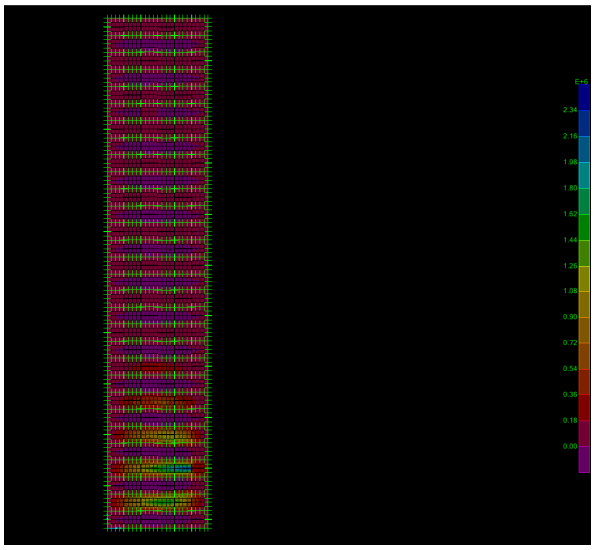

Figure 65. Distribution of the buckling Load stresses

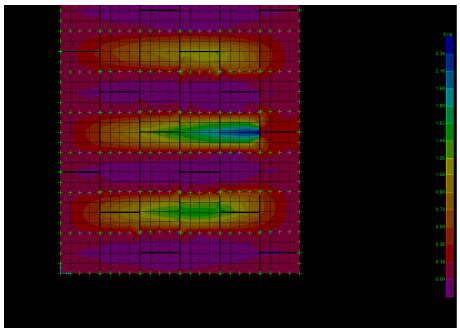

Figure 66. A zoom of the stresses

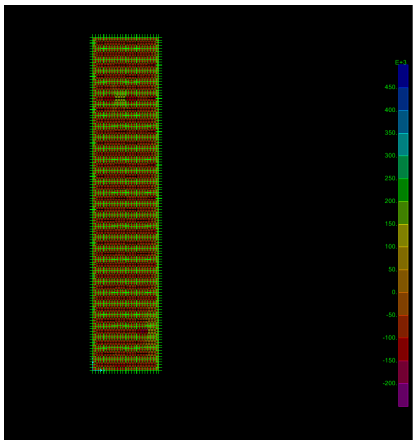

Figure 67. Distribution of live load stresses

The stresses increase in the connections between the panels. The tolerance used for the welds is of 0.2 m because the gap is 0.1m and to have the effect of continuity the tolerance must be higher than the gap.

To verify if the connections works as continuous between the panels I chose 2 joints in the x and y directions

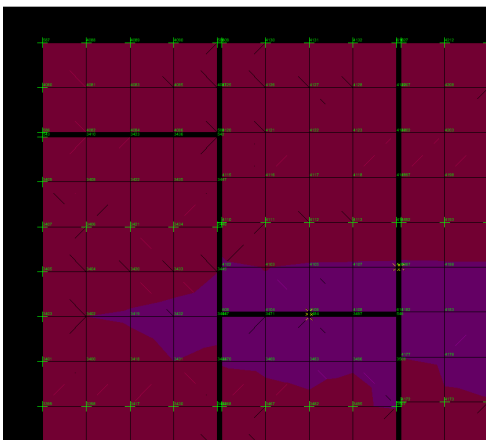

Figure 68. Detail of the stresses at the staggered interconnections

Then I looked at their displacements and rotations, as shown in the table below.

Horizontal joints

Joint	case	U1 m	U2 m	U3 m	R1 Radians	R2 Radians	R3 Radians
3484	L	4.051E-08	-0.00028	0	0	0	-5.5E-08
3484	BUCK1	0	0	-1.7E-07	7.82E-09	1.24E-08	0
3484	BUCK1	1.454E-19	0	0.000342	-7.5E-06	-3.4E-05	1.9E-20
3484	BUCK1	0	0	0.000121	-2.2E-07	-1.3E-05	0
3484	BUCK1	-1.038E-13	2E-14	-0.00004	-1.9E-07	4.34E-06	1.42E-15
3484	BUCK1	1.039E-13	4.06E-14	-0.00026	-5.4E-06	0.00003	1.66E-14
3484	BUCK1	3.832E-14	1.09E-14	0.000581	-1.6E-05	9.97E-06	-3.6E-14
4106	L	4.601E-08	-0.00028	0	0	0	-5.5E-08
4106	BUCK1	0	0	-1.7E-07	7.82E-09	1.24E-08	0
4106	BUCK1	1.435E-19	0	0.000341	-7.5E-06	-3.4E-05	1.9E-20
4106	BUCK1	0	0	0.000121	-2.2E-07	-1.3E-05	0
4106	BUCK1	-1.039E-13	2E-14	-0.00004	-1.9E-07	4.34E-06	1.42E-15
4106	BUCK1	1.022E-13	4.06E-14	-0.00026	-5.4E-06	0.00003	1.66E-14
4106	BUCK1	4.192E-14	1.09E-14	0.000579	-1.6E-05	9.97E-06	-3.6E-14

Table 1. Displacements and rotations in two coincident joints

Vertical Joints

Joint	OutputCase	U1	U2	U3	R1	R2	R3
		m	m	m	Radians	Radians	Radians
4109	L	5.193E-09	-0.000284	0	0	0	-6.735E-08
4109	BUCK1	0	0	-1.255E-07	0.000000103	3.41E-10	0
4109	BUCK1	1.178E-19	0	0.000277	-0.00022	-0.000015	-9.93E-20
4109	BUCK1	0	0	0.000101	-0.000079	-0.000006694	0
4109	BUCK1	-8.558E-14	-6.677E-15	-0.000034	0.000026	0.00000232	-8.573E-15
4109	BUCK1	2.175E-13	-3.039E-14	-0.000225	0.000171	0.000017	-1.324E-13
4109	BUCK1	6.948E-14	5.482E-15	0.000341	-0.000266	0.000092	-8.659E-15
4187	L	5.193E-09	-0.000284	0	0	0	-6.735E-08
4187	BUCK1	0	0	-1.255E-07	0.000000103	3.41E-10	0
4187	BUCK1	1.178E-19	-1.153E-20	0.000279	-0.00022	-0.000015	-9.93E-20
4187	BUCK1	0	0	0.000102	-0.000079	-0.000006694	0
4187	BUCK1	-8.558E-14	-7.534E-15	-0.000034	0.000026	0.00000232	-8.573E-15
4187	BUCK1	2.175E-13	-4.363E-14	-0.000227	0.000171	0.000017	-1.324E-13
4187	BUCK1	6.948E-14	4.616E-15	0.000332	-0.000266	0.000092	-8.659E-15

Table 2. Displacements and rotations in two coincident joints

I can conclude that the displacements and rotations are equal for each pair of joints, so the continuity assumption is respected.

Now I continued with the same procedure as in the other cases to see how the structure buckles getting off 1, 2, 3, 4 floors and look what happened.

Lost 1 floor

λcr =8.6

$$Pc1 = 8.6 \cdot 12.25 = 105 \ KN/m$$

which is a reduction of the 38% of the buckling capacity Pc

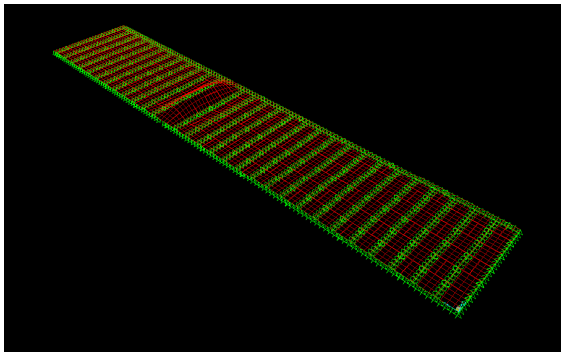

Figure 69. Buckling mode shape

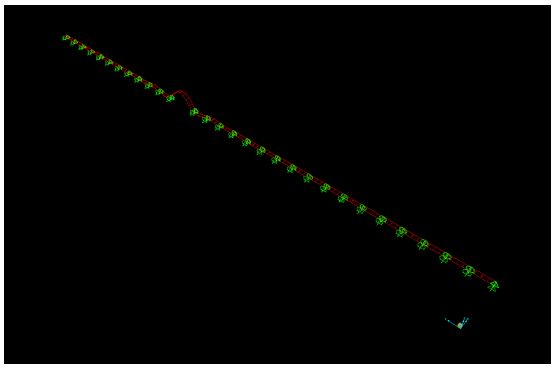

Figure 70. Line selection of the buckling mode shape

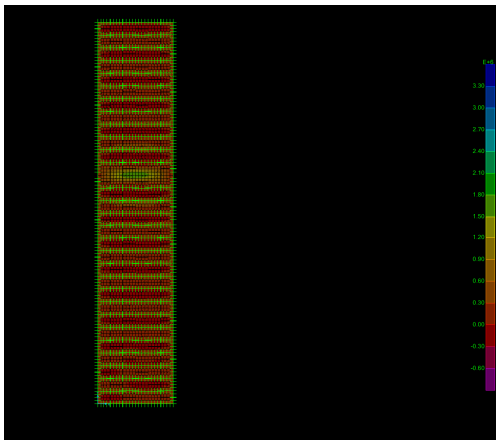

Figure 71. Distribution of buckling load stresses

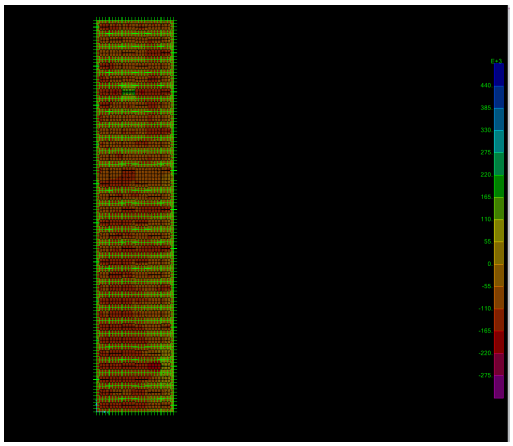

Figure 72. Live load stresses

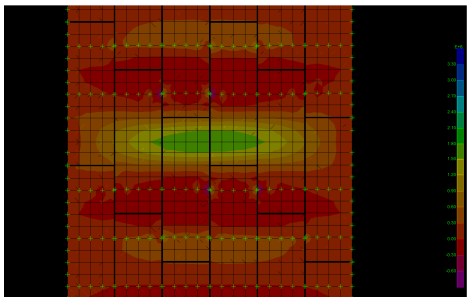

Figure 73. A zoom of the stresses in the floor collapsed

The tensile stresses are concentrated in the middle and the compression stresses are near the supports. Close to the connections of the panels there isn't a different distribution of stresses because they are continuous.

Lost 2 floors

λcr= 4.7

$$Pc2 = 4.7 \cdot 12.25 = 57.6 \ KN/m$$

which is a reduction of the 66% of the buckling capacity Pc

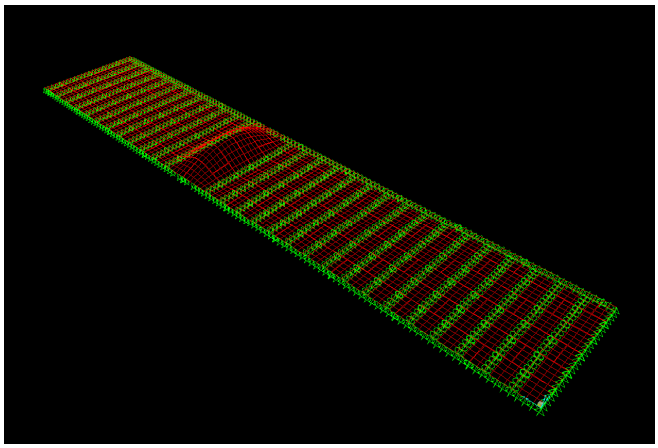

Figure 74. Buckling mode shape

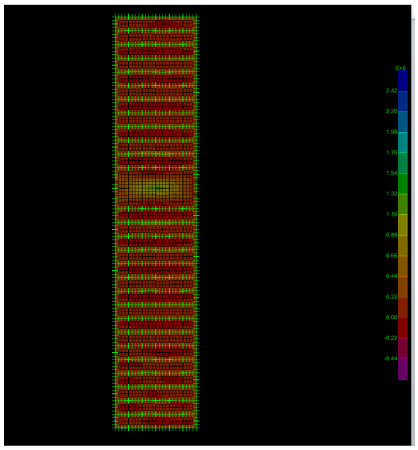

Figure 75. Distribution of the buckling stresses

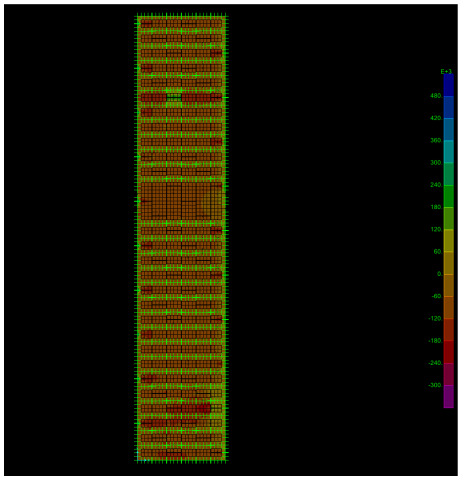

Figure 76. Live load stresses

From this figure is possible to see that the tensile stresses decrease and increase the compression stresses.

Lost 3 floors

λcr= 3

$$Pc3 = 3 \cdot 12.25 = 37 \ KN/m$$

which is a reduction of the 79% of the buckling capacity Pc

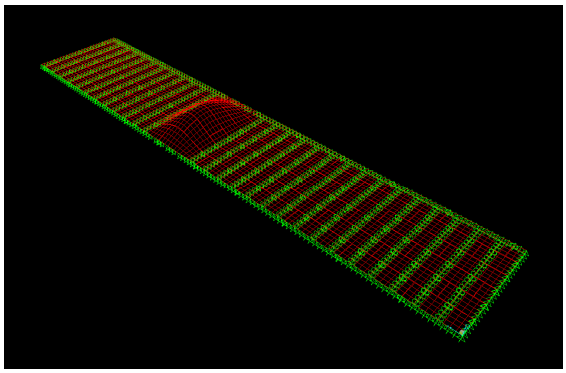

Figure 77. Buckling mode shape

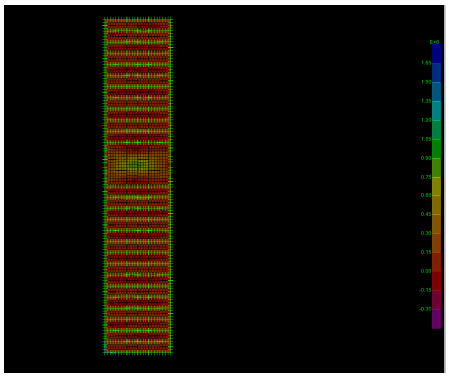

Figure 78. Distribution of the buckling stresses

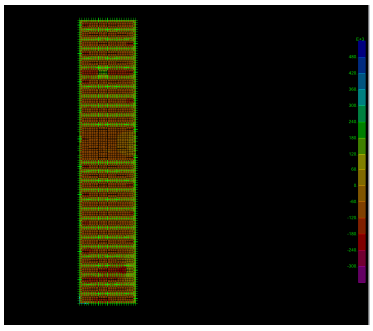

Figure 79. Live load stresses

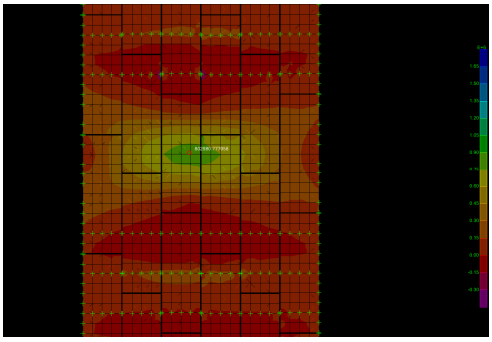

Figure 80. A zoom of the stresses in the failure zone

The compression stresses increase spreading inside in the middle of the floor while the tensile stresses become more concentrated in the center of the floor.

Lost 4 floors

λcr=2.2

$$Pc4 = 2.2 \cdot 12.25 = 27 \ KN/m$$

which means a reduction of the 86% of the buckling capacity Pc

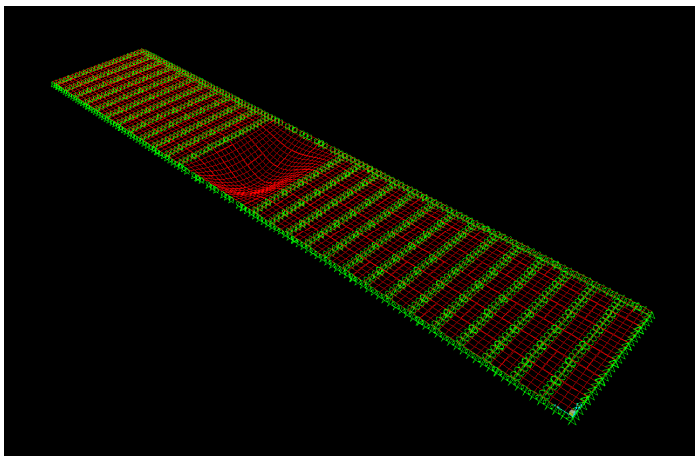

Figure 81. Buckling mode shape

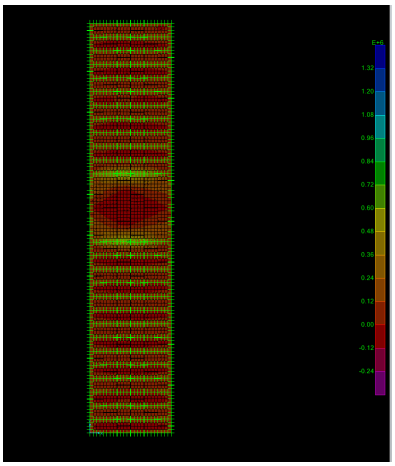

Figure 82. Distribution of the buckling load stresses

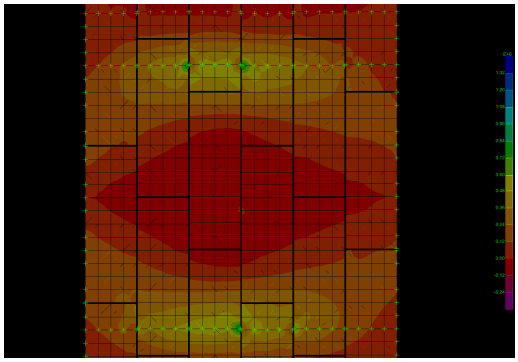

Figure 83. A zoom of the stresses

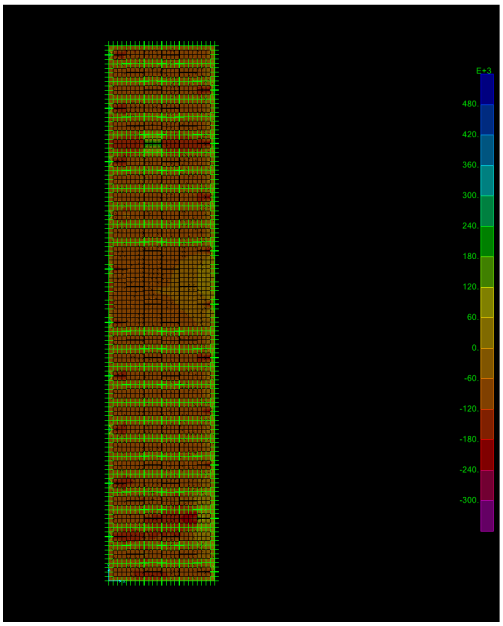

Figure 84. Live load stresses

The compression stresses are concentrated in the middle of the floor and there are no tensile stresses, which are now concentrated near the supports.

4.5 Case 2 Hinged panels

Now I wanted to see the difference of buckling capacity in the case in which all the panels were continuous and the case of the hinged panels. The presence of hinges affected significantly the buckling capacity of the wall but removing the floors the reduction of the buckling capacity doesn't differ too much from the continuous case. This means that the reduction of the buckling capacity doesn't affected the collapse of the structure but it is due to the strength of the connection and to the loss of the support of the floors.

This one is the last case I studied, which is the one closer to the structure of the Twin Towers. In this case I put the condition of continuity between the panels only in the vertical direction and in the horizontal direction, I put the hinges as follows:

Vertical boundary condition between panels		Horizontal boundary conditions	
Ux1=Ux2	Rx1=Rx2	Ux1=Ux2	Rx1≠Rx2
Uy1=Uy2	Ry1=Ry2	Uy1=Uy2	Ry1=Ry2
Uz1=Uz2	Rz1=Rz2	Uz1=Uz2	Rz1=Rz

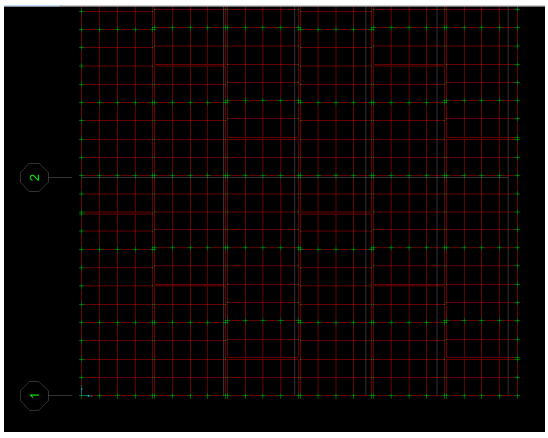

Figure 85. Vertical welds between the panels

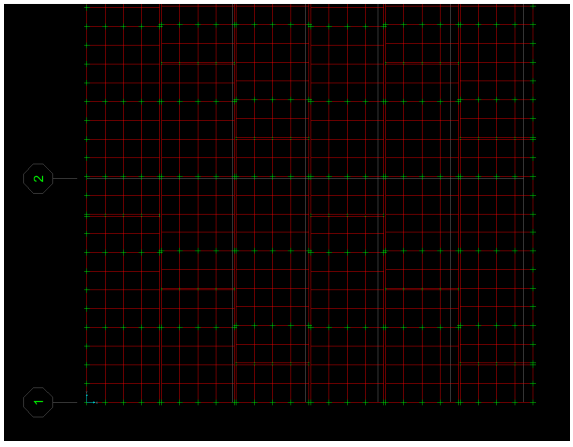

Figure 86. Horizontal welds between the panels

Horizontal constraints

Joint	CaseType	U1	U2	U3	R1	R2	R3
		m	m	m	Radians	Radians	Radians
3484	LinStatic	-1.2E-08	-0.00027	0	0	0	-4.5E-07
3484	LinBucklin	0	0	-0.00089	-0.00048	0.000049	0
3484	LinBucklin	0	0	0.001094	0.00059	6.3E-06	0
3484	LinBucklin	0	0	0.000124	0.000068	4.01E-07	0
3484	LinBucklin	1.17E-16	-5.3E-17	0.001315	0.00074	7.16E-06	6.57E-17
3484	LinBucklin	1.51E-16	-4.4E-17	0.00174	0.00099	0.000015	-5.2E-19
3484	LinBucklin	-1E-16	2.49E-17	0.000616	0.000358	0.000013	9.04E-17
4106	LinStatic	3.32E-08	-0.00027	0	0	0	-4.5E-07
4106	LinBucklin	0	0	-0.00089	0.000488	0.000049	0
4106	LinBucklin	0	0	0.001094	-0.00061	6.3E-06	0
4106	LinBucklin	0	0	0.000124	-6.8E-05	4.01E-07	0
4106	LinBucklin	1.11E-16	-5.3E-17	0.001315	-0.00072	7.16E-06	6.57E-17
4106	LinBucklin	1.51E-16	-4.4E-17	0.00174	-0.00095	0.000015	-5.2E-19
4106	LinBucklin	-1.1E-16	2.49E-17	0.000616	-0.00033	0.000013	9.04E-17

Table 3. Displacements and rotations of two coincident joints

The conditions are all satisfied, in fact the only one which is different is the rotation in the x axis. All the other displacements and rotations are the same in the 2 coincident joints.

Vertical constraints

Joint	CaseType	U1	U2	U3	R1	R2	R3
	Text	m	m	m	Radians	Radians	Radians
4109	LinStatic	-7.364E-09	-0.000274	0	0	0	1.204E-07
4109	LinBuckling	0	0	-0.000394	0.000389	0.000054	0
4109	LinBuckling	0	0	0.000336	-0.000359	0.000114	0
4109	LinBuckling	0	0	0.00004	-0.000041	0.00001	0
4109	LinBuckling	2.549E-16	-6.227E-17	0.000427	-0.000433	0.000097	-2.474E-16
4109	LinBuckling	1.331E-16	-3.765E-17	0.000563	-0.000564	0.000124	-3.826E-17
4109	LinBuckling	-5.671E-17	2.163E-17	0.000195	-0.000188	0.000042	-2.015E-17
4187	LinStatic	-7.364E-09	-0.000274	0	0	0	1.204E-07
4187	LinBuckling	0	0	-0.0004	0.000389	0.000054	0
4187	LinBuckling	0	0	0.000325	-0.000359	0.000114	0
4187	LinBuckling	0	0	0.000039	-0.000041	0.00001	0
4187	LinBuckling	2.549E-16	-8.7E-17	0.000417	-0.000433	0.000097	-2.474E-16
4187	LinBuckling	1.331E-16	-4.148E-17	0.00055	-0.000564	0.000124	-3.826E-17
4187	LinBuckling	-5.671E-17	1.961E-17	0.000191	-0.000188	0.000042	-2.015E-17

Table 4. Displacements and rotations of two coincident joints

Also from this table it is possible to see that the conditions are satisfied because the displacements and the rotations are the same for each joint.

Now I run the linear buckling analysis and I obtained the following results:

λcr= 7.8

$$Pr = 7.8 \cdot 12.25 = 95.5\ KN/m$$

which is a reduction of the 44%of the buckling capacity Pc in the continuous case

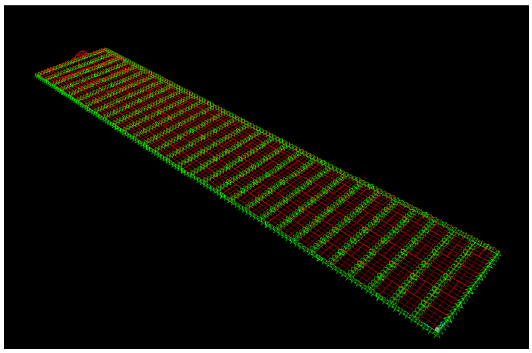

Figure 87. Buckling mode shape

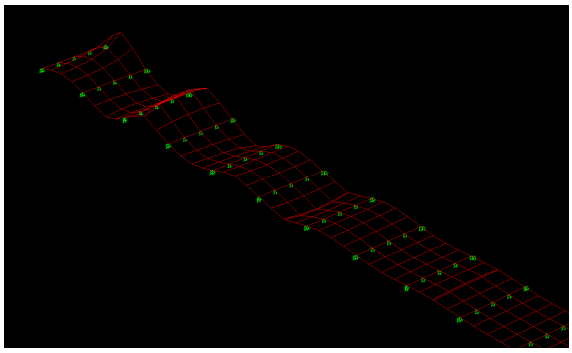

Figure 88. Line selection of the buckling mode shape

The critical load is lower than the continuous case because of the presence of the horizontal hinges. The buckling capacity is almost half than that one in the continuous case, in fact Pr: 95.5KN which represents a reduction of the 46 % of the critical load in the continuous case (Pc=169KN).

But when I will go to get off the floors the ratio of the buckling load doesn't change very much. It doesn't buckle faster than the continuous case.

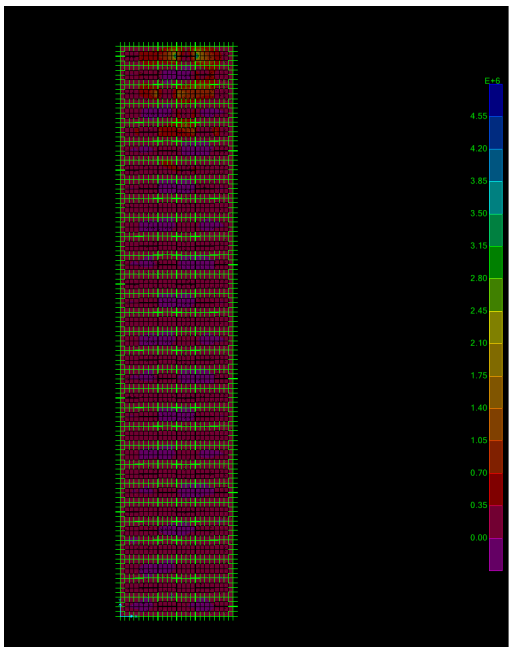

Figure 89. Distribution of the buckling loads Stresses

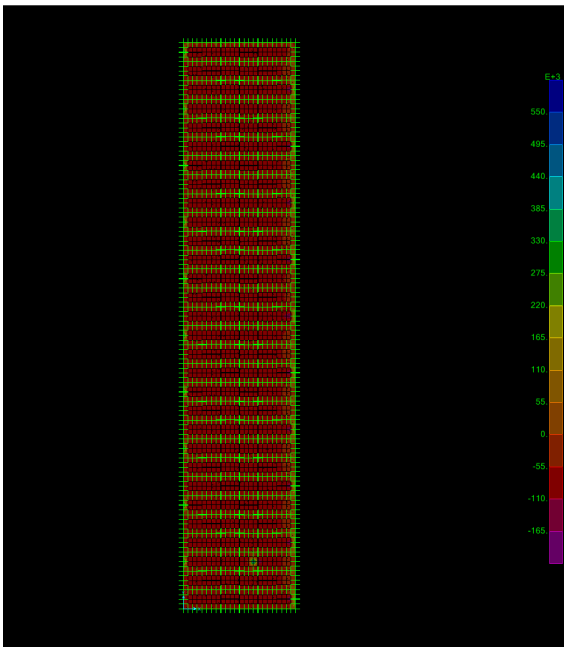

Figure 90. Live load stresses

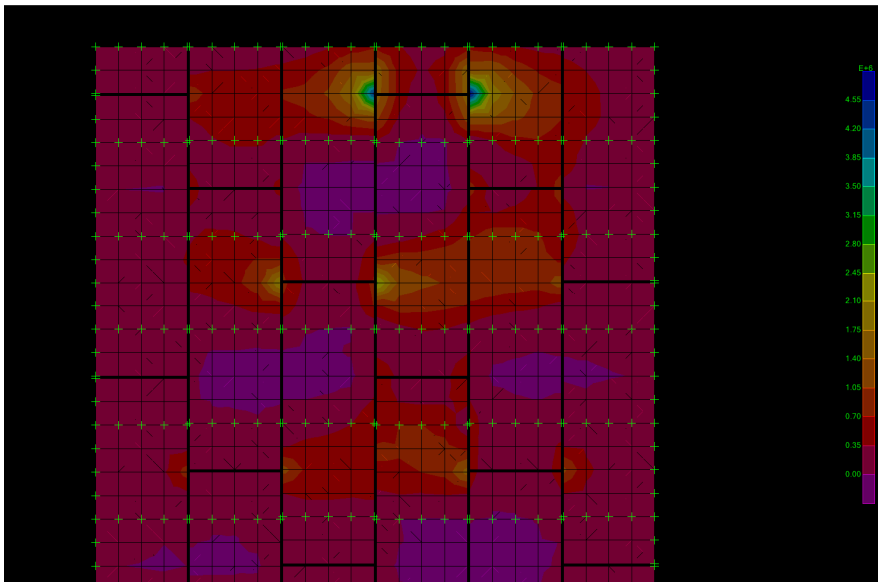

Figure 91. A zoom of the stresses

The distribution of the stresses decreases from the top to the bottom. The stresses are more different than in the other cases because of the hinges between the panels. There is an alternation of compressive and tensile stresses. The tensile stresses are concentrated at the corner of the panels and the compressive stresses are in the middle of two adjacent panels.

Lost 1 floor

λcr= 6.7

$$Pr1 = 6.7 \cdot 12.25 = 82\ KN/m$$

which is a reduction of the 15% of the buckling capacity Pr.

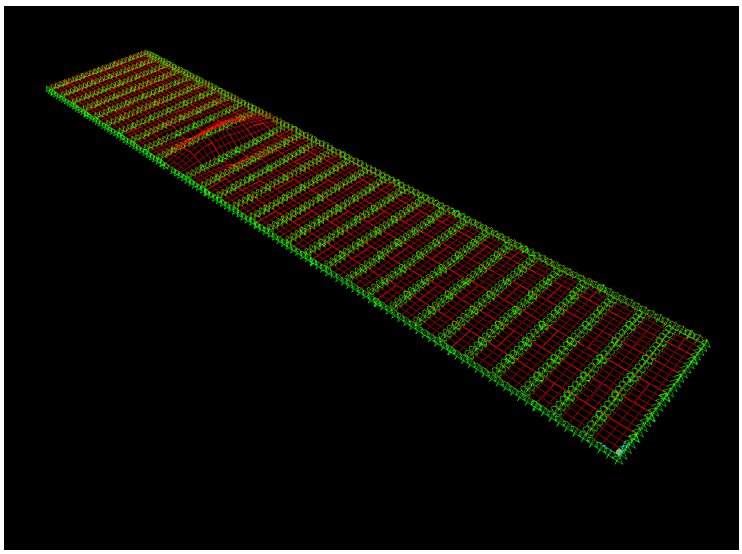

Figure 92. Buckling mode shape

This value isn’t too lower than that one in the continuous case, so the hinges don’t affect too much the buckling capacity of the floors. The hinges affect significantly the buckling capacity of the wall but not too much the capacity of the floors.

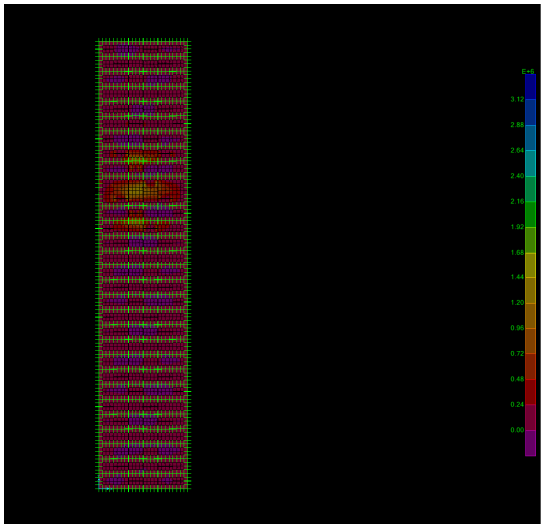

Figure 93. Distribution of the buckling load stresses

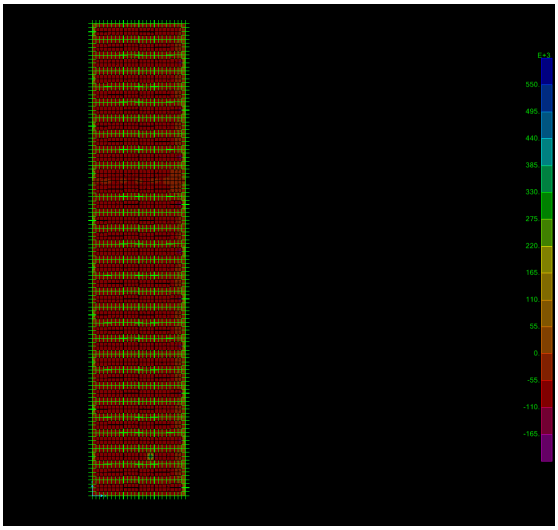

Figure 94 Live load stresses

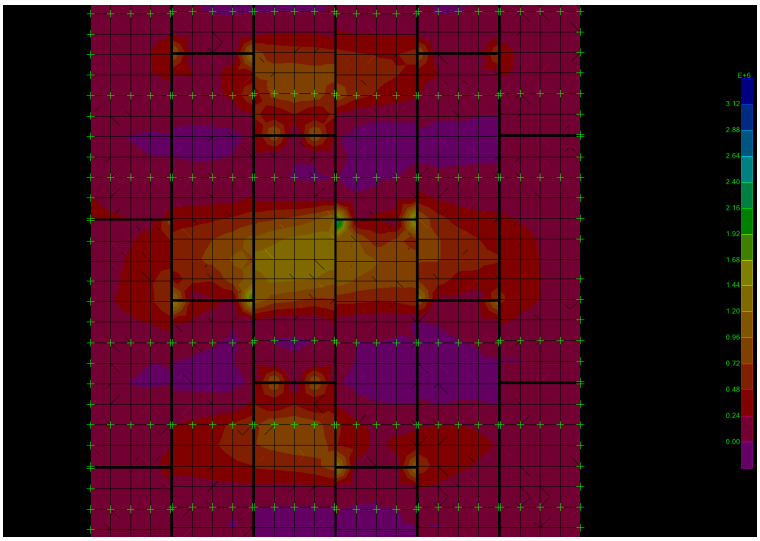

Figure 95. A zoom of the stresses

Almost all the tensile stresses are concentrated in the damaged part of the structure, in the middle between the two floors and the compression stresses are spread symmetrically along the height of the plate

Lost 2 floors

λcr= 3.8

$$Pr2 = 3.8 \cdot 12.25 = 46.5\ KN/m$$

which is a reduction of the 51% of the buckling capacity Pr

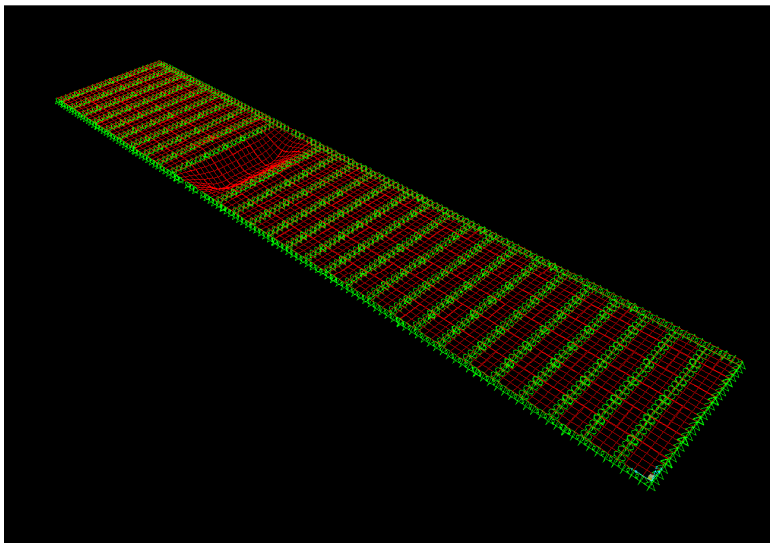

Figure 96. Buckling mode shape

Removing another floor the ratio of the buckling decreases. Now the ratio is of 0.56Pr. So the biggest difference is getting of 1 floor than it buckles slowly.

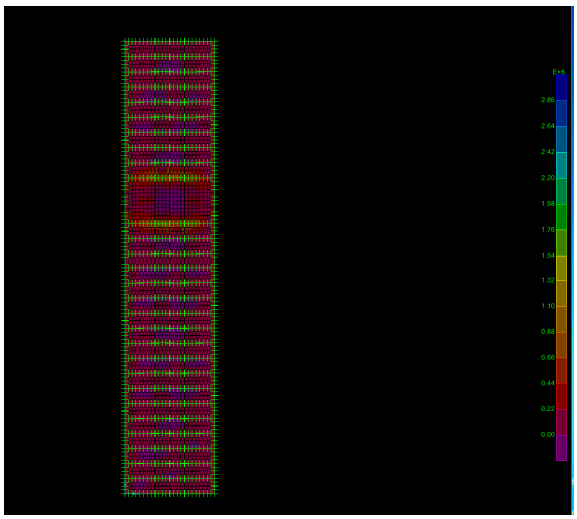

Figure 97. Buckling load stresses

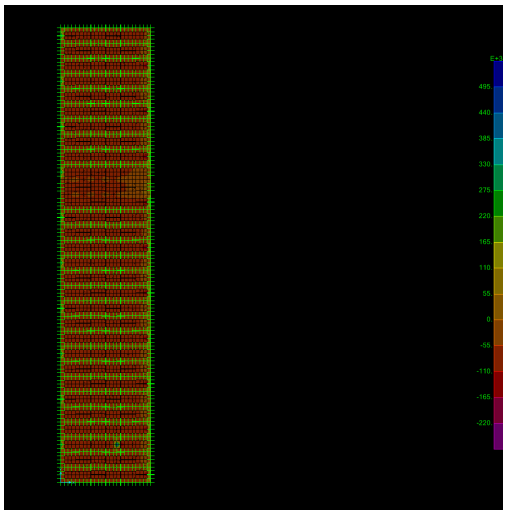

Figure 98. Live load stresses

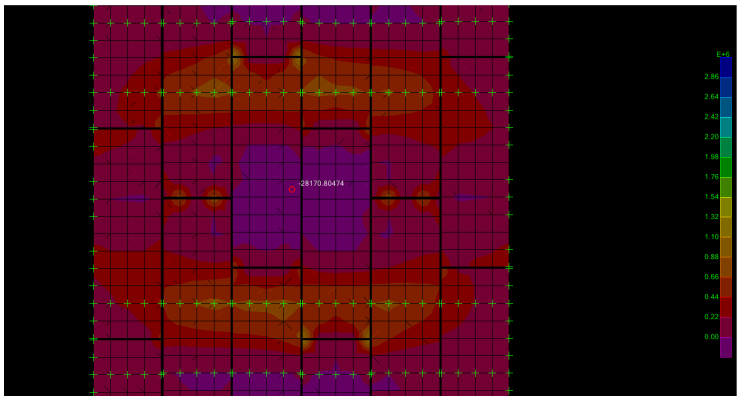

Figure 99. Stresses in the failure zone

The distribution of the stresses is changed. In the center of the central panels there are compression stresses but near the connections and near the supports there are tensile stresses.

Lost 3 floors

λcr= 2.5

$$Pr3 = 2.5 \cdot 12.25 = 30.6KN/m$$

Which is a reduction of the 68% of the buckling capacity Pr

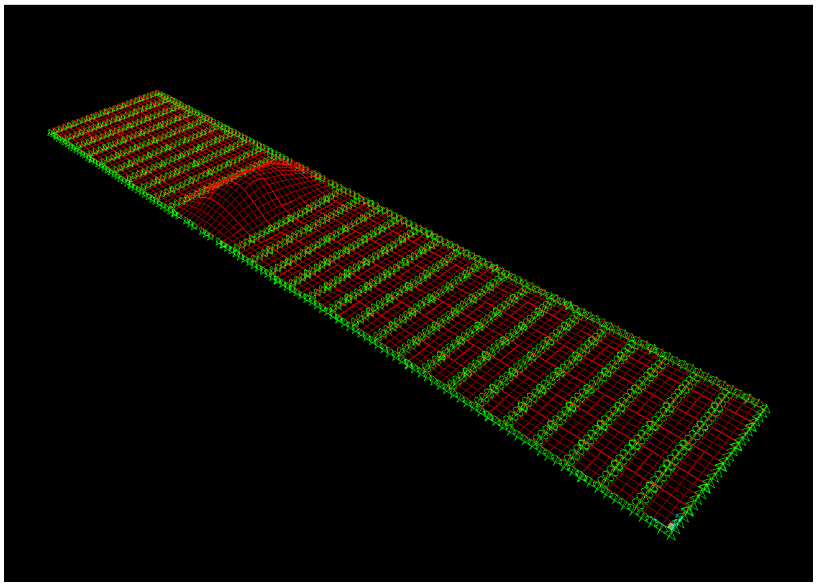

Figure 100. Buckling mode shape

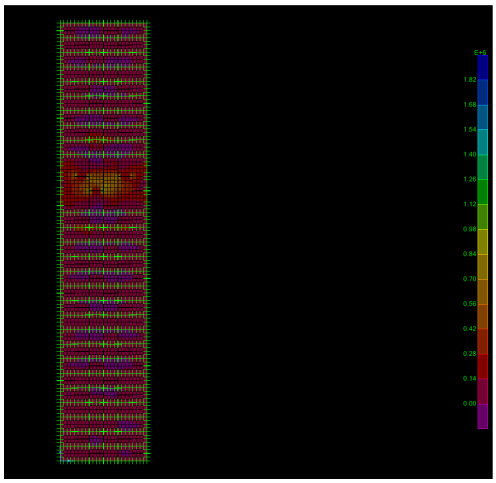

Figure 101. Distribution of the stresses

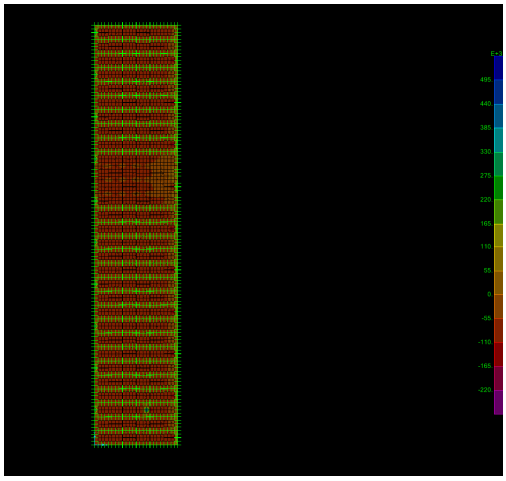

Figure 102. Distribution of the live load stresses

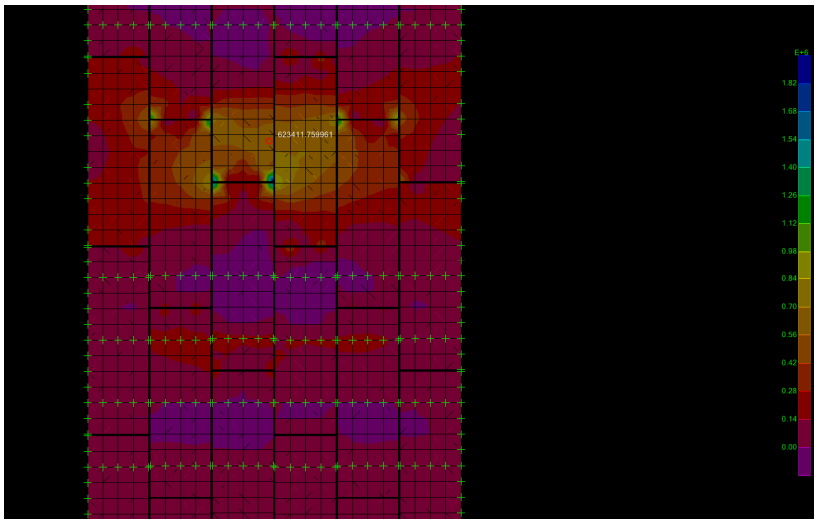

Figure 103. A zoom of the stresses

The tensile stresses starting from the edge of the connections are increased, spreading between the two floors, with the higher value in the center. The compression stresses are more concentrated near the supports of each floor

Lost 4 floors

λcr=1.8

$$Pr4 = 1.8 \cdot 12.25 = 22\ KN/m$$

Pr=18 KN which is a reduction of the 77% of the buckling capacity Pr

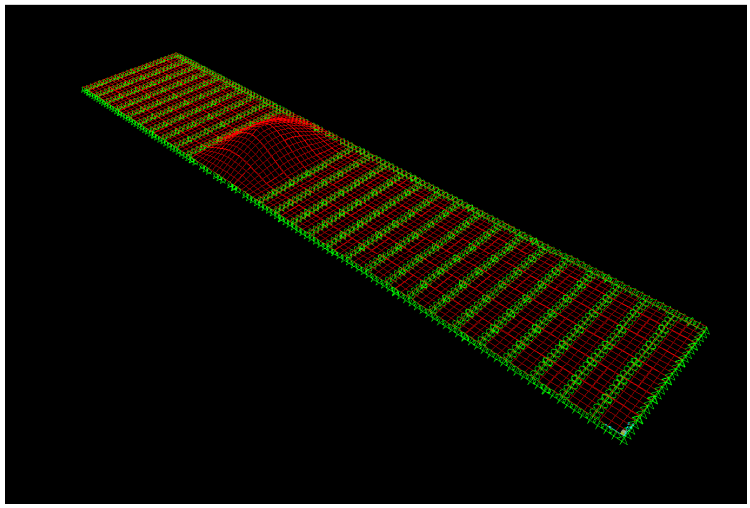

Figure 104. Buckling mode shape

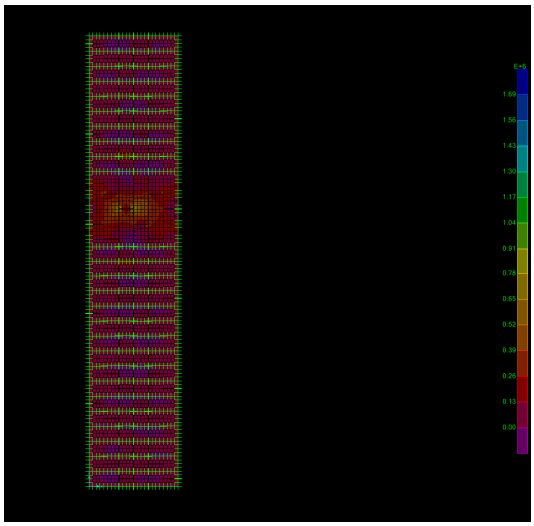

Figure 105. Distribution of the buckling load stresses

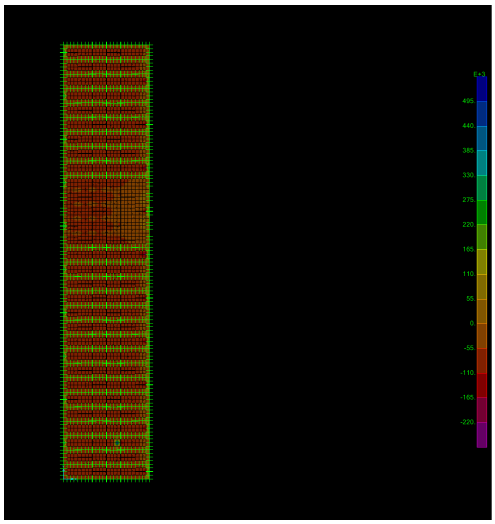

Figure 106. Live load stresses

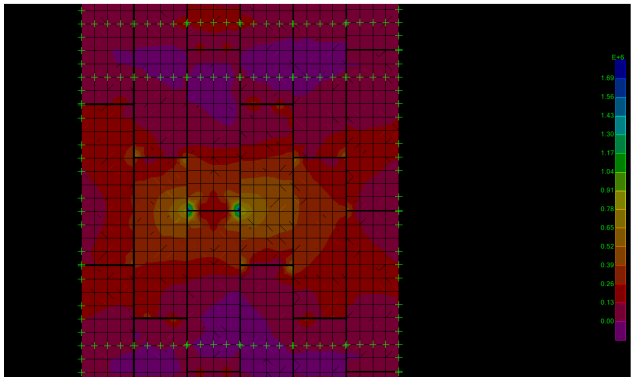

Figure 107. A zoom of the stresses

The distribution of stresses isn't so different from the last one. The tensile stresses starting from the edges of the panels are spread in the middle of the floors. The compression stresses are more concentrated near the supports.

Below I reported a table to summarize the results obtained in the 2 cases

	Continuous panels	Hinged panels
Pcr	169 KN/m	95.5 KN/m
Pcr1	105 KN/m	82 KN/m
Pcr2	57.6 KN/m	46.5 KN/m
Pcr3	37 KN/m	30.6 KN/m
Pcr4	27 KN/m	22 KN/m

Chapter 5 Discussion of the results

After the obtained results I wanted to check if the analysis performed were good because I hadn't anything to compare with it. To do it I made small plates with different conditions. First of all I made a continuous plate with continuous panels because I wanted to see how much the value of the critical load changes in this case compared with one, with only horizontal welds and another one with only vertical welds. I also studied for each model the orthotropic and isotropic case. The Orthotropic plate has different axial and bending stiffness in the x and y directions. The Isotropic plate has the same stiffness in the 2 directions.

This table below is a brief summary of the results:

	Orthotropic model	Isotropic model
Horizontal central welds	113 KN/m	161 KN/m
Horizontal lateral welds	126 KN/m	168 KN/m
Vertical welds	143 KN/m	160 KN/m
Vertical welds on the lower right side	137 KN/m	161 KN/m
Continuous plate	144 KN/m	174 KN/m

For each plate I used the following properties:

Material

Steel A992Fy50

E: 199999 Mpa

Poisson ratio: 0.3

Width=6 meters

Heigth=12 meters

Gap= 0.1 m

Tol=0.2m

Panels dimensions:

Width=2 m

Heigth= 6 m

Reference load:

$$Po = \frac{7 \cdot 1}{6} = 1.16\ KN/m$$

Axial stiffness in the x direction/Axial stiffness in the y direction= 0.5

Bending stiffness in the x direction/bending stiffness in the y direction= 0.1

5.1 Case 1

a. Orthotropic continuous plate

I started with the continuous plate and after this I compared the critical load with the same plate but with isotropic behavior. I will see that the difference in the stiffness affects the value of the critical load, there is a reduction of the 18% of the buckling load compared with the isotropic case (Pc=174 KN/m)

The value of the critical load is:

λcr= 124

$$Pc = 124 \cdot 1.16 = 144\ KN/m$$

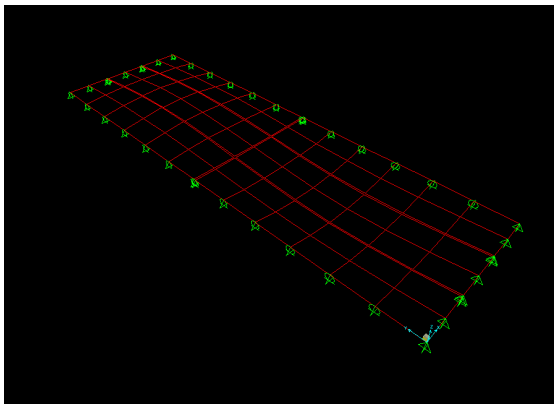

Figure 108. Buckling mode shape – continuous orthotropic plate

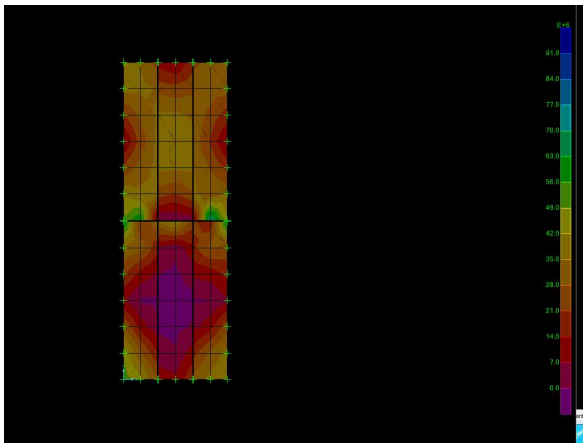

Figure 109. Distribution of the buckling load stresses

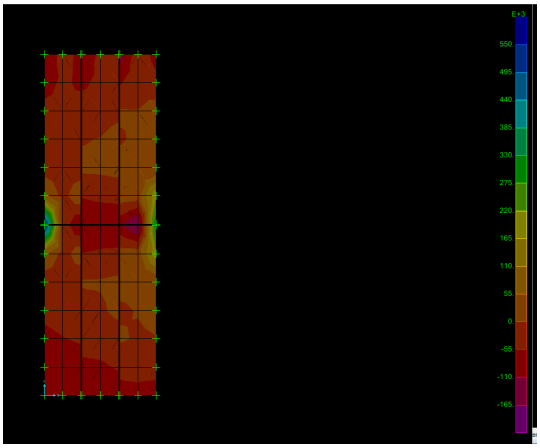

Figure 110. Distribution of live load stresses

The compressive stresses are concentrated at the bottom of the plate and the maximum value is achieved in the central panel. The tensile stresses achieve their maximum in the

central panel in the upper part of the plate. The distribution of the stresses is comparable with the one of the continuous panels (compression and tensile stresses alternated at each floor)

b. Isotropic continuous plate

The isotropic plate, with the same stiffness in the 2 perpendicular directions, shows a higher value of the critical load.

λcr=150

$$Pc = 150 \cdot 1.16 = 174\ KN/m$$

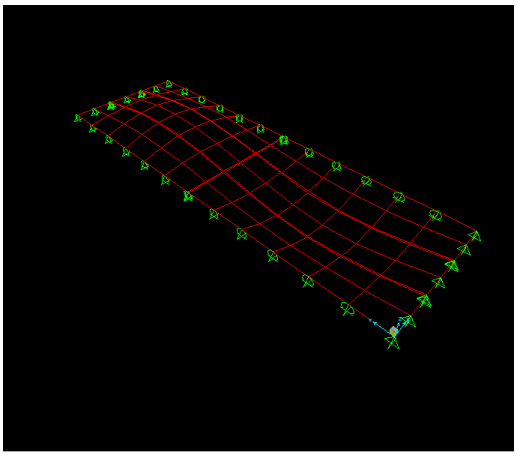

Figure 111. Buckling mode shape-isotropic plate

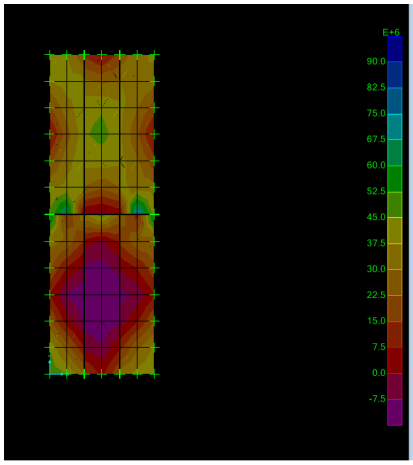

Figure 112. Buckling load stresses

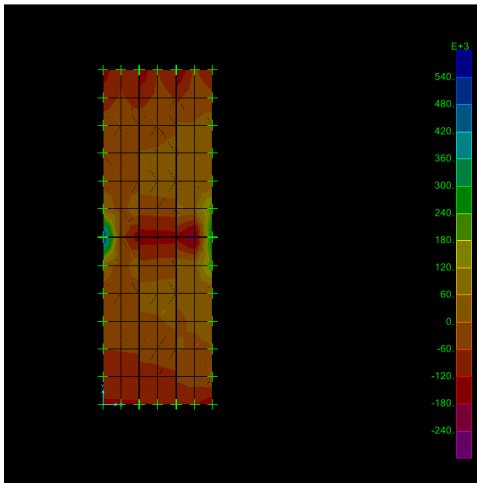

Figure 113. Live load stresses

The compressive stresses are also in this case concentrated in the bottom of the plate and in particular in the central panel. The tensile stresses reach their maximum in the top central panel.

5.2 Case 2

a. Isotropic plate with Vertical welds

In this model I put the vertical welds in the upper left panel. In the other entire panel the welds are continuous. The results obtained are little bit lower than the continuous plate and present a reduction of the 9% of the buckling load Pc(174KN/m). This means that the introduction of the hinges in the model doesn't affect too much the buckling capacity.

Vertical welds conditions on the upper left panel

Ux1=ux2	Rx1=Rx2
Uy1=uy2	Ry2≠Ry2
Uz1=uz2	Rz1=Rz2

λcr=138

$$Pr = 138 \cdot 1.16 = 160\ KN/m$$

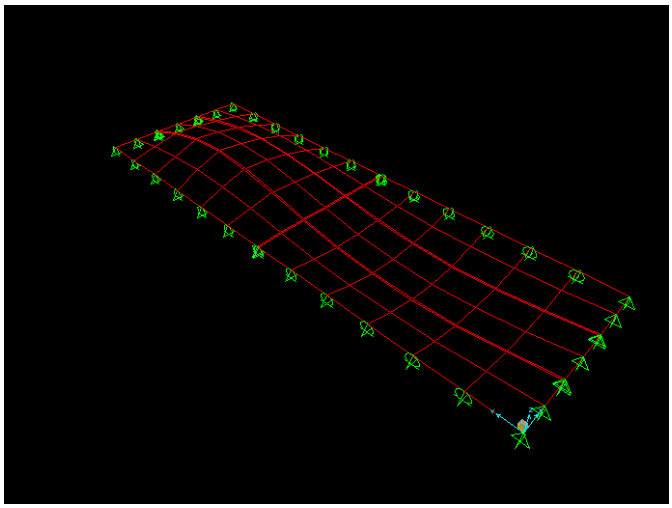

Figure 114. Buckling mode shape-isotropic plate

The presence of the hinges doesn't change too much the value of the critical load. This explains the result obtained in the study performed, which means that the weak connections doesn't affect significantly the reduction of the buckling capacity.

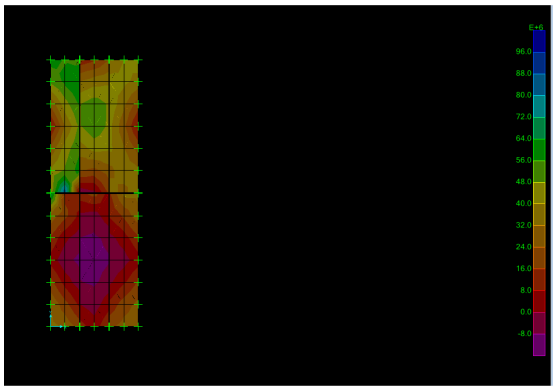

Figure 115. Buckling load stresses

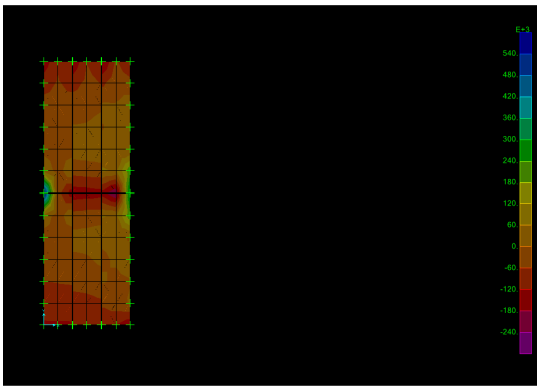

Figure 116. Live load stresses

The distribution of the stresses is almost the same as the continuous plate. In the bottom there are compressive stresses and in the top tensile stresses.

b. Orthotropic plate with vertical welds

In this case the critical load is lower than the previous one because the plate is orthotropic with different axial and bending stiffness in the 2 perpendicular directions and the value is:

λcr= 123

$$Pr = 123 \cdot 1.16 = 143\ KN/m$$

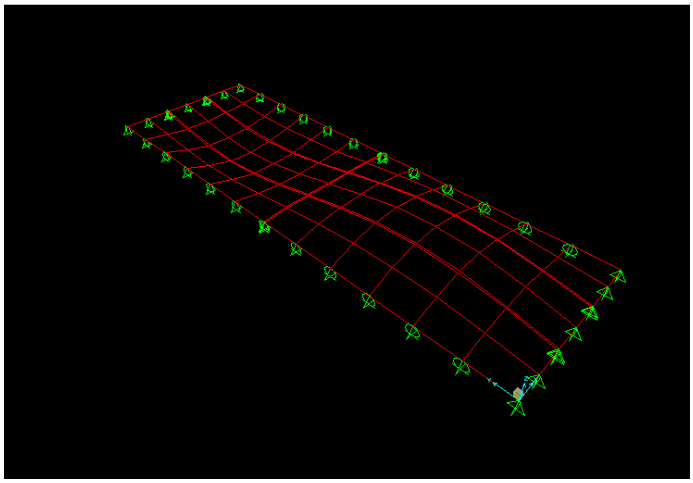

Figure 117. Buckling mode shape-orthotropic plate

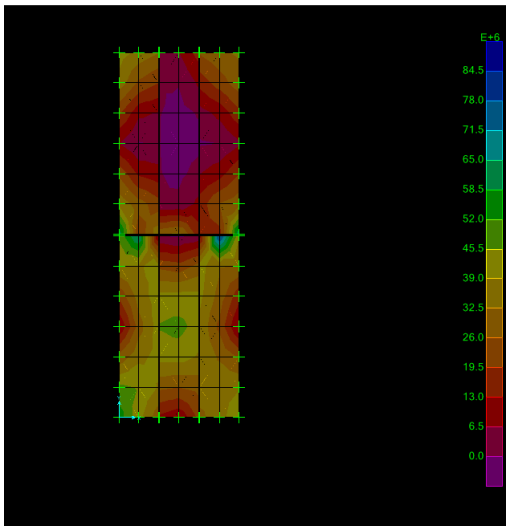

Figure 118. Buckling stresses

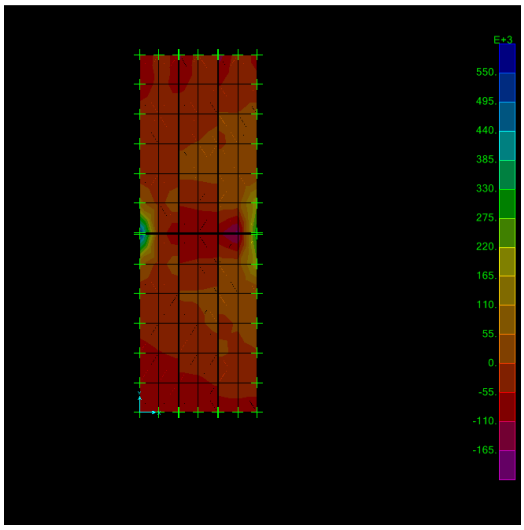

Figure 119. Live load stresses

The distribution of the stresses is the opposite of the isotropic case.

c. Isotropic plate with vertical welds on the lower right side

In this case I considered the same plate but with the vertical welds in the lower right side. In this way I wanted to see if the critical load changed. The value is little bit different because in the case with the welds in the upper side the value was 174 KN/m and here is 161KN/m. This difference is due to the different restraints in the top and in the bottom of the plate. The hinges in different position don't change too much the critical load, so the model is good.

The critical load is

λcr=139

$$Pr = 139 \cdot 1.16 = 161\ KN/m$$

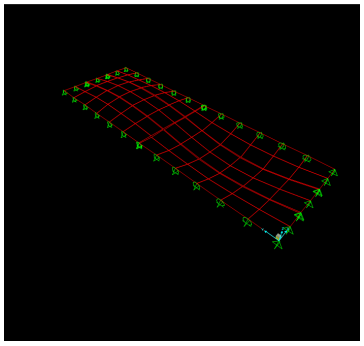

Figure 120. Buckling mode shape-isotropic plate

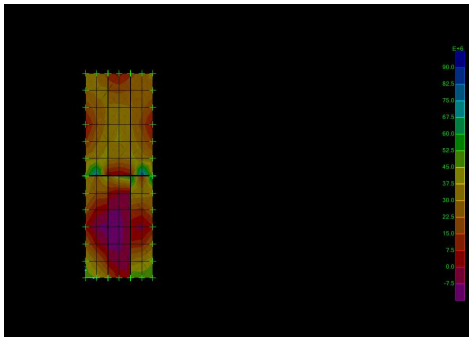

Figure 121. Buckling stresses

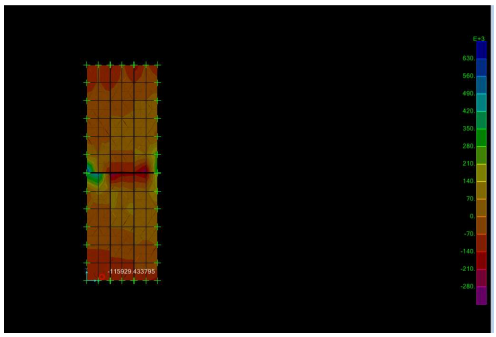

Figure 122. Live load stresses

d. Orthotropic plate with vertical welds on the lower right side

Now I studied the same plate but orthotropic. This change causes a lower value of the critical load and consequently the structure buckles with a smaller critical load.

The critical load is:

λcr=118

$$Pr = 118 \cdot 1.16 = 137\ KN/m$$

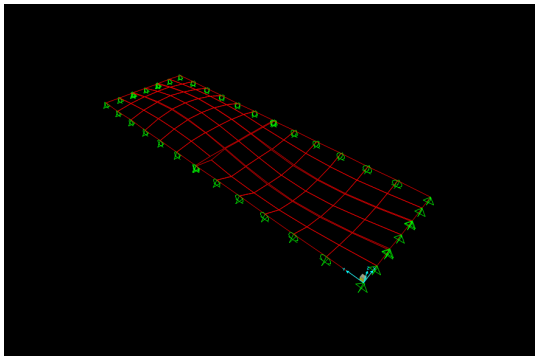

Figure 123. Buckling mode shape – orthotropic plate

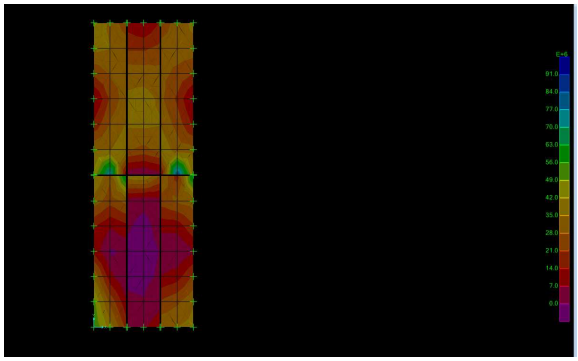

Figure 124. Buckling stresses

The distribution of the stresses is almost the same as the previous case.

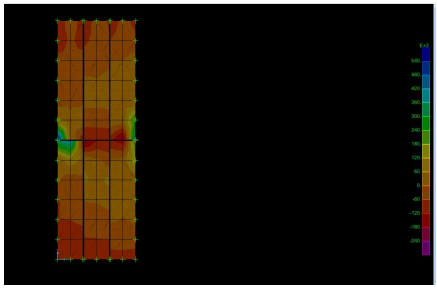

Figure 125. Live load stresses

5.3 Case 3

a. Orthotropic Plate with Horizontal central welds

Now I considered the hinges in the horizontal edge of the panel as in the simplify model studied in which the hinges are only in the horizontal edge of the panels. The other properties remain the same and I started taking into consideration the different stiffness in the 2 directions and then I considered the cases with isotropic behavior in the x and y directions and with the hinges not in the central panel but in the lateral one. I compared this value with the results of the continuous plate. In this case the horizontal welds boundary conditions are:

Ux1=ux2 Rx1≠Rx2

Uy1=uy2 Ry1=Ry2

Uz3=uz3 Rz3=Rz3

The obtained value of the critical load differs from the buckling load in the continuous plate Pc (144.6KN). In the real structure the presence of the hinges affected the buckling capacity of the wall but the weaker connections aren't the main cause of the collapse because the reduction of the buckling capacity when the floors are removed doesn't dramatically reduces. This means that the collapse is affected by the loss of the bracing of the floors

λcr=97

$$Pr = 97 \cdot 1.16 = 113\ KN/m$$

Which is 0.78Pc in the continuous case

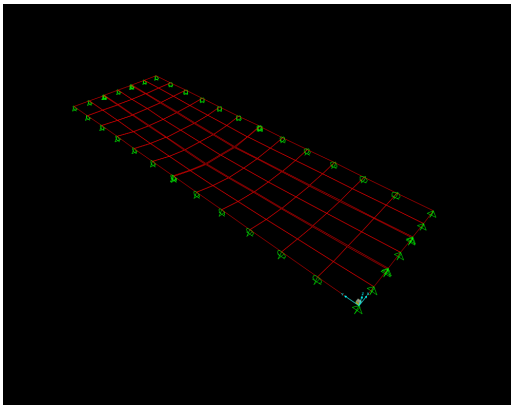

Figure 126. Buckling mode shape-orthotropic plate

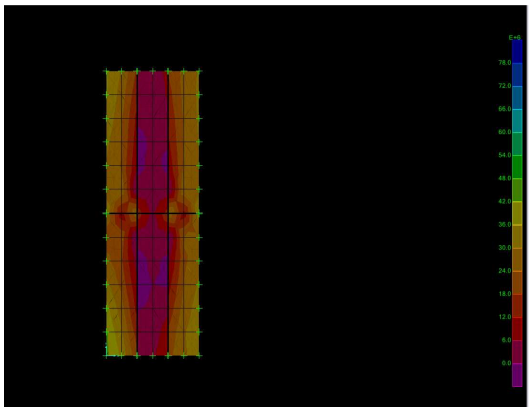

Figure 127. Buckling load stresses

The compressive stresses are concentrated in the center of the plate. The weakness of the connections is due to the high compressive stresses.

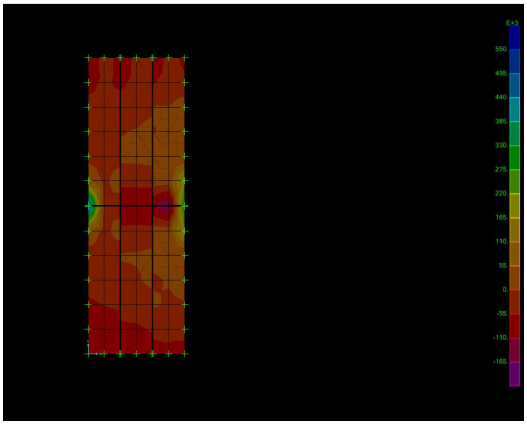

Figure 128. Live load stresses

c. Isotropic plate with horizontal central welds

In this case I considered the same plate but isotropic, with the same stiffness in both directions. This is another verification that with the same stiffness in the two perpendicular directions the value of the buckling load is higher, so the stiffness is a factor that affects the stability of the structure.

The value of the critical load is:

λcr=140

$$Pr = 140 \cdot 1.16 = 161\ KN/m$$

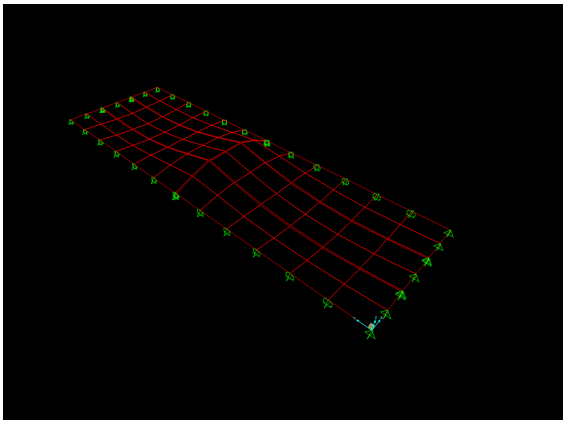

Figure 129. Buckling mode shape- isotropic plate

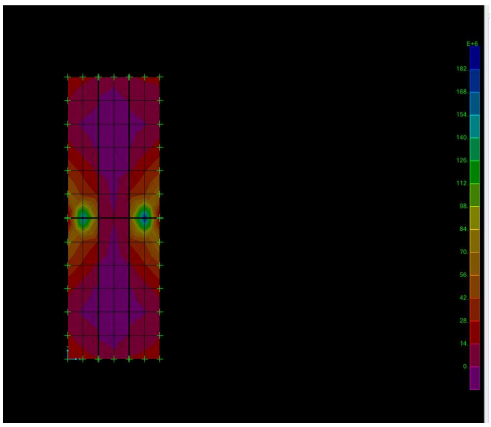

Figure 130. Buckling load stresses

The distribution of the stresses is the same as in the other case. Near the horizontal hinges there are tensile stresses and the compressive stresses are concentrated in the center of the top and bottom of the plate

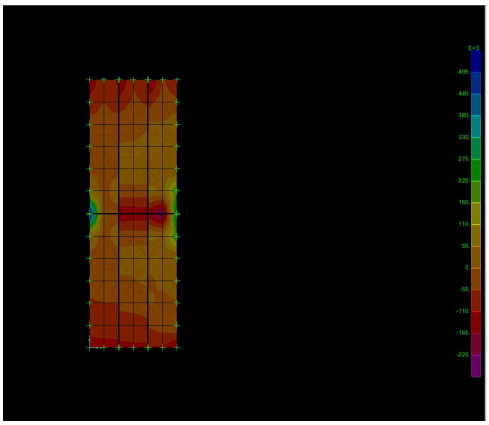

Figure 131. Live load stresses

d. Orthotropic plate with lateral horizontal welds

In this case I studied the same plate but with the horizontal hinges in the lateral side and not in the center. In this case the value of the critical load is different from the previous one because I put the hinges only in two joints and not in 3 joints as before because in the lateral side there are the restraints. For this reason the value is lower.

The critical load is:

λcr=109

$$Pr = 109 \cdot 1.16 = 126\, KN/m$$

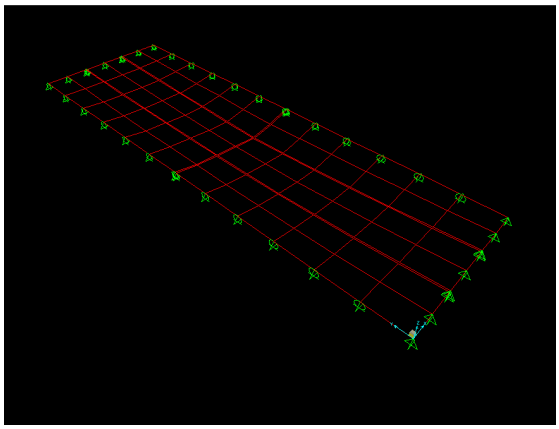

Figure 132. Buckling mode shape – orthotropic plate

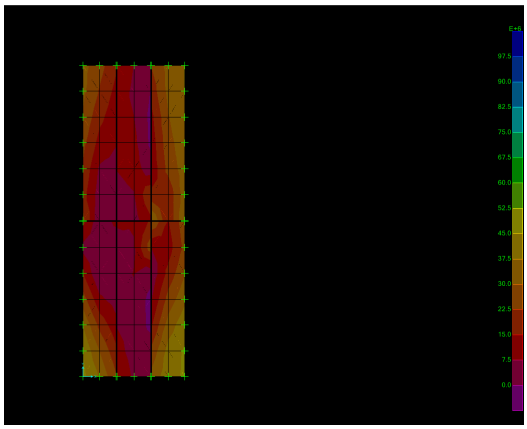

Figure 133. Buckling load stresses

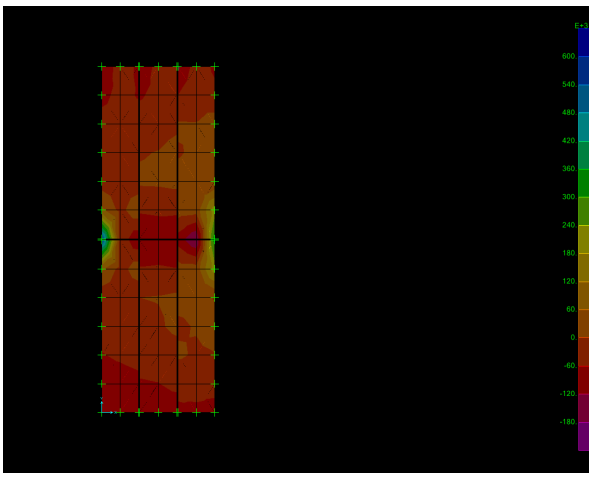

Figure 134. Live load stresses

e. Isotropic plate with horizontal welds on the other side

In this model I considered the same stiffness in both directions. The value of the critical load is also in this case higher than the previous one because of the change in the axial and bending stiffness. This is another proof that the changes in the stiffness bring to a lower value of the critical load.

The critical value is:

λcr=145

$$Pr = 145 \cdot 1.16 = 168\ KN/m$$

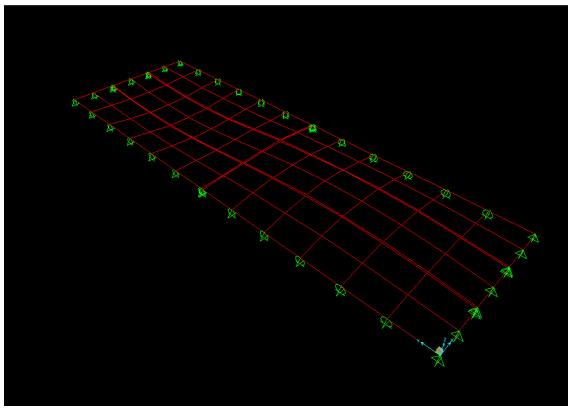

Figure 135. Buckling mode shape- isotropic plate

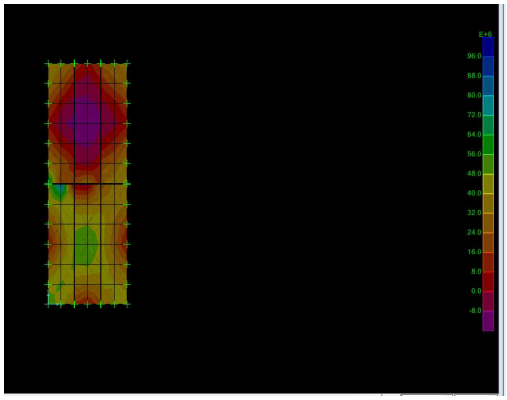

Figure 136 Buckling load stresses

The distribution of the stresses is similar to the other case. The compressive stresses are at the top of the structure and the tensile stresses are in the bottom reaching their maximum value in the central panel.

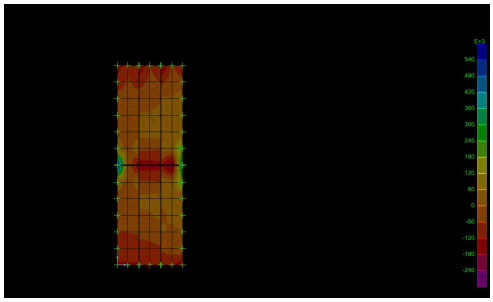

Figure 137. Live load stresses

These simple cases studied, allow saying that the presence of the hinges affects the buckling capacity of the wall but not dramatically. In the study performed we saw that buckling capacity isn't affected by the weaker interconnections between the panels.

Conclusion

The floors in the Twin Towers provided lateral support for the walls of the outer tube at each floor level. The loss of that bracing for the tube perimeter walls when floors collapsed greatly reduced the buckling capacity of the walls and their ability to carry the weight above. It was thought that the staggered interconnections between panels comprising the tube walls might have introduced weaknesses that further reduced the buckling capacity after the loss of bracing from the floor, but the results of this analysis show that it was not a significant factor.

A Simplified model was analyzed to investigate the influence of the staggered interconnections between the panels. Two main cases were considered:

In the first case the Panels as orthotropic plates were connected rigidly to represent one wall of the tube; in the second case the same panels, with the extreme case of moment releases at the staggered connections, to represent an extreme condition.

This study shows that the loss of bracing from the collapse of successive floors significantly reduces the buckling capacity of the continuous wall. The buckling capacity of the wall with continuous panels is Pc: and it decreases when it is lost the bracing of the floors. The ratios of the buckling capacity of the removed floors, Pc_1, Pc_2, Pc_3, Pc_4, over the buckling capacity of the wall, Pc, is 0.62, 0.34, 0.22 and 0.16 respectively.

Comparing this case with moment releases at panel joints, the buckling capacity of the wall is also significantly affected, showing a value of the critical load Pr reduced to 0.54Pc, which implies a 46% reduction of the buckling capacity in the continuous case. However for the case of the loss of one, two, three and four floors, critical load, Pr_1, Pr_2, Pr_3, Pr_4 Pr reduced to 0.85, 0.49, 0.32, 0.23 respectively.

The results obtained from the 2 different cases (the plate with continuous panels and the one with hinged panels) show that when the structure loses the support of the floors, the critical buckling load decreases with almost the same ratio in the 2 cases. This means that although the panel interconnections, considered here as the extreme condition of hinged connections, do affect the buckling capacity of the tube significantly, the

reduction in buckling capacity that results from loss of support from the floors is not reduced to any great extent.

The analysis shows that the perimeter wall, lost the lateral support of the floors, buckled and the weaker connections between the panels didn’t contribute to the reduction of the buckling capacity as supposed initially. The weaker joints between panels are reflected in the eventual failures of those joints during the collapse so that the panels could be clearly identified in the rubble.

In conclusion, from the study performed follows that the main factor which brings to the entirely collapse of the buildings is the loss of the lateral support of the floors. In fact when one floor buckles it falls on the floor below giving it an additional load. The floor can’t carry an additional load and this is why it falls down on the other floor. This process continues as a chain of events until all the structure collapses.

References

[1] Ronald Hamburger, William baker, Jonathan Barnett, James Mike, Harold “Bud” Nelson. *Fema report2002* http://911research.wtc.net/mirrors/guardian/wtc/WTC_ch2.htm

[2] Eduard Ventsel, Theodor Krauthammer *Thin Plates and Shells* Theory, Analysis and Applications, The Pennsylvania State University, University park, Pennsylvania Marcell Dekker, Inc. 2001

[3] Computers and Structures, Inc. Berkeley, California, USA. Version 7.0 Revised 1998 *Sap2000 Integrated Finite Element Analysis and Design of Structures*. Analysis Reference.

[4] *“The World Trade Center Tube”* Tube.HowStuffWorks

[5] *Linear Buckling Analysis* http://www.kxcad.net/Altair/Hyper.Works/oshelp/linear_buckling_analysis

Acknowledgements

It is a pleasure to thank those who made this thesis possible. I would like to thank Professor Marco Savoia who taught me and enabled me to make my thesis abroad. I am grateful to Professor Rene B. Testa who gave me the opportunity to prepare my thesis at Columbia University. With his enthusiasm and his great efforts to explain things clearly and simply he helped me to write this thesis. It was an honor for me to study in this prestigious University and I would like to thank all the people in the Civil Engineering department of Columbia University. I want to show my gratitude to the Ph.D. supervisor, Arturo Montoya. Throughout my thesis, he provided encouragement, good teaching, and lots of good ideas. I would like to thank all the Professors of my Course of study in the University of Bologna. I am grateful to all the friends and people of the International House in New York for providing a stimulating and fun environment in which I spent 6 beautiful months. I wish to thank my family for supporting me and providing a loving environment for me.